MODELING REACTION KINETICS OF CHLORINE DIOXIDE AND VOLATILE

ORGANIC COMPOUNDS WITH ARTIFICIAL NEURAL NETWORKS

by

CHENG HU

(Under the Direction of R. W. McClendon and J. R. Kastner)

ABSTRACT

Increasing public concerns over odors and air regulations in non-attainment zones necessitate the remediation of a wide range of volatile organic compounds (VOCs) generated in the poultry-rendering industry. Currently, wet scrubbers using oxidizing chemicals, such as chlorine dioxide (ClO_2), are applied to remove VOCs. However, little information is available on the kinetics of chlorine dioxide reaction with rendering air pollutants, which limits wet scrubber design and optimization. Kinetic analysis indicated that chlorine dioxide does not react with aldehydes under typical conditions, while thiols and disulfides rapidly reacted with chlorine dioxide. Moreover, pH can affect their reaction rates significantly. In order to obtain the kinetic data without the study of their complex reaction mechanisms, artificial neural networks (ANNs) were used to model the reactions of chlorine dioxide and VOCs. For the oxidation of single VOC, a standard three-layer back-propagation ANN was developed to predict the reaction rates. For VOC mixtures, a Ward ANN provided the best performance. The final models can be used to predict the initial ClO_2 reaction rates with ethanethiol or DMDS for the design and optimization of wet scrubbers.

INDEX WORDS: Chlorine dioxide, volatile organic compounds, reaction kinetics, artificial neural network, modeling

MODELING REACTION KINETICS OF CHLORINE DIOXIDE AND VOLATILE

ORGANIC COMPOUNDS WITH ARTIFICIAL NEURAL NETWORKS

by

CHENG HU

B.S., Xi'an Institute of Science & Technology, China, 1993

Ph.D., Dong Hua University, China, 1998

A Thesis Submitted to the Graduate Faculty of The University of Georgia in Partial Fulfillment

of the Requirements for the Degree

MASTER OF SCIENCE

ATHENS, GEORGIA

2003

MODELING REACTION KINETICS OF CHLORINE DIOXIDE AND VOLATILE

ORGANIC COMPOUNDS WITH ARTIFICIAL NEURAL NETWORKS

by

CHENG HU

Major Professor:	R. W. McClendon
Committee:	J. R. Kastner
	W. D. Potter

Electronic Version Approved:

Maureen Grasso
Dean of the Graduate School
The University of Georgia
December 2003

ACKNOWLEDGEMENTS

TABLE OF CONTENTS

LIST OF TABLES

LIST OF FIGURES

CHAPTER 1

INTRODUCTION

The promulgation of "Odor Control Rules", increasing public concerns, and EPA air regulations in non-attainment zones necessitate the remediation of a wide range of volatile organic compounds (VOCs) generated in the rendering industry. Currently, wet scrubbers using oxidizing chemicals, such as ClO_2 are utilized to treat VOCs. However, little information is available on the kinetics of ClO_2 reactions with rendering air pollutants, which limits wet scrubber design and optimization (Kastner and Das, 2002).

The overall goal of our research is to study the chemical reaction kinetics of chlorine dioxide and VOCs, to model the reactions using artificial neural networks, and to provide a kinetic basis for the design and optimization of web scrubbers and potentially develop process control methodologies.

In Chapter 2, an experimental study was performed to determin if chlorine dioxide would react with straight chain and branched aldehydes, recently identified in rendering emissions. The kinetics of chlorine dioxide reaction with rendering air pollutants was also studied. Two model compounds, ethanethiol and dimethyl disulfide (DMDS) were selected for the kinetic study. Besides reaction orders, reaction rate constants, the effect of pH and temperature on the reaction rate were determined. A wet scrubber model utilizing the kinetic data was developed to predict scrubber performance.

Artificial neural networks (ANNs) have been intensively in chemistry and drug design in recent years (Zupan and Gasteiger, 1999). In Chapter 3, we used ANNs to model the reactions of chlorine dioxide with single VOC compound (ethanethiol and DMDS individually) without the study of the reaction mechanisms. To use the experimental data efficiently, k-fold cross validation was adopted to develop and evaluate ANN models. Through the selection of suitable network architectures and network parameter optimization, a standard three-layer feed-forward ANN with back-propagation learning algorithm was developed for the modeling.

In Chapter 4, experiments of the reaction of chlorine and VOC mixtures were designed and data were acquired in a spectrophotometer with an automatic stopped flow system. Based on the experimental data, a more complex neural network model, the Ward net, was used to predict the reaction rate of chlorine dioxide with VOC mixtures.

Conclusions and future work have been summarized in Chapter 5.

REFERENCES

Kastner, J. K., and Das, K. C., 2002. Wet scrubber analysis of volatile organic compound removal in the rendering industry. *Journal of the Air & Waste Management Association*, 52, 459-469.

Zupan, J., and Gasteiger, J. (1999). *Neural networks in chemistry and drug design*. Weinheim: Wiley-Vch.

CHAPTER 2

KINETICS AND MODELING OF ODOR OXIDATION USING CHLORINE DIOXIDE FOR

EMISSION CONTROL WITH WET SCRUBBERS

2.1 INTRODUCTION

Poultry rendering operations convert organic wastes to products such as feed additives

and fertilizer. In poultry rendering operations feathers are typically hydrolyzed in batch mode to

breakdown the keratin (Prokop, 1974) and the meat by-products or offal are typically treated

batch or continuous, with varying residence times depending on the mode of operation (Prokop,

1985 and 1991). In some cases, the hydrolyzed feathers are then combined with offal and dried.

In both of these steps, volatile organic compounds (VOCs) are generated, some of which are

odorous. Overhead vapors from the feather hydrolyser and driers are passed through condensers

to remove some VOCs. The non-condensables are typically passed through wet scrubber units to

remove the VOC fraction not removed in the condensers.

Venturi scrubbers, packed-bed wet scrubbers, and biofilters have been used for odor

removal in the rendering industry (Prokop, 1991). Venturi and packed-bed wet scrubbers are

sometimes coupled together since the Venturi is a single stage scrubber (i.e., limited mass

transfer capabilities) and acts to reduce temperature at particulate levels. A variety of oxidizing

chemicals have been used as oxidizing agents, including sodium hypochlorite, chlorine gas,

chlorine dioxide (ClO_2), and ozone/NaOCl (Prokop, 1991). Removal efficiencies based on odor

units ranged from 99% to 93-96% for processes using a Venturi and a packed-bed wet scrubber (water and NaOCl) and a single packed-bed system (ClO_2) treating low intensity odors, respectively (Prokop, 1991). However, design data, such as optimum chemical concentration, were not reported. Moreover, removal efficiencies were based on odor units, which give no indication of individual and total VOC removal efficiencies.

For poorly, water soluble VOCs, mass transfer from the gas phase must be coupled with rapid reaction in the liquid phase for high removal efficiencies in wet scrubbers. Thus, removal efficiencies will depend not only on Henry's Law, but on the reaction rate and order in the liquid film. It is theorized that chemical oxidizing agents react with many of the odor causing compounds in rendering emissions (e.g., H_2S, methanethiol). Recently, major compounds consistently identified in rendering emissions included dimethyl disulfide, methanethiol, octane, hexanal, 2-methylbutanal, 3-methylbutanal, and 2-methylpropanal (Kastner and Das, 2002). The two branched aldehydes, 2-methylbutanal and 3-methylbutanal, were typically the largest fraction of the VOC mixture. Hexanal, 2-methylbutanal, and 3-methylbutanal have been associated with negative odor properties and chemical smells (Brewer et al., 1999; Hrudey et al., 1988). Hexanal has been identified as the primary odor causing compound in the overuse of frying oil and the branched aldehydes associated with wastewater odors. However, kinetic data specific for the VOCs generated in the rendering industry is lacking, without which optimal scrubber design is impractical (Overcamp, 1999). Kinetic data suggest that typical oxidizing agents used in wet scrubbers (e.g., ClO_2 and ozone) do not react or react slowly with many of the VOCs in rendering plant waste gases (Rav-Acha and Choshen, 1987; Hoigne and Bader, 1994), however, the kinetics of reaction between ClO_2 (and other oxidizing agents) with the major VOC fractions in rendering emissions has not been measured. Reaction rate constants ranging from 4 x

10^4 to 3×10^8 (L/mol/s) are reportedly required to achieve rapid removal in wet scrubbers (Overcamp, 1999). Benzaldehyde, a representative aldehyde periodically measured in rendering emissions (Barnes and MacLeod, 1982) has a reported reaction rate constant of less than 3×10^{-4} (L/mol/s) with ClO_2 (Hoigne and Bader, 1994). Thus, critical data are lacking to assess and design wet scrubbers for total VOCs.

The objectives of this research were to determine if ClO_2 would react with straight chain and branched aldehydes recently identified in rendering emissions, and to determine the kinetics of ClO_2 reaction with rendering air pollutants, and develop a wet scrubber model utilizing the kinetic data to predict scrubber performance. These data will provide a basis for lowering VOC emissions (both odorous and ozone contributing) via process improvements.

2.2 MATERIALS AND METHODS

2.2.1 Chemicals

All chemicals were of reagent grade and ethanethiol, 2-methylbutyraldehyde, and hexanal were obtained from Aldrich. Dimethyl disulfide was obtained from Acros Organics. All buffer solutions were prepared at 0.2M and included sodium acetate-acetic acid (pH 3.6), sodium phosphate dibasic-sodium phosphate monobasic (pH 6.9), and carbonate-bicarbonate (pH 9 and 11.02). Chlorine dioxide was prepared in a SVP-Pure^{TM} Chlorine Dioxide Generator (EKA Chemicals Inc.) and the chemical reaction used to generate chlorine dioxide was the following (Tenney, 1997):

$$NaClO_3 + 1/2\ H_2SO_4 + 1/2\ H_2O_2 \rightarrow ClO_2 + 1/2\ O_2 + 1/2\ Na_2SO_4 + H_2O \qquad (1)$$

The chlorine dioxide solution, typically ranging in concentration from 2.0-2.1 g/L, was stored at 4°C up to 4 months before use. The maximum absorbance wavelength for ClO_2 was confirmed to be 358 nm via manual scanning and the molar absorptivity was calculated by measuring absorbance at 358 nm at several different concentrations (6-60 mg/L) and found to be 1195 L mol^{-1} cm^{-1}. Chlorine dioxide concentrations were confirmed using the iodometric method (Greenberg et al., 1992).

2.2.2 Kinetic analysis

2.2.2.1 Rate law

Experiments were designed such that the volatile organic compound (e.g., 2-methylbutanal) was in excess relative to ClO_2 and the rate law could be considered pseudo-first-order (Hoigne and Bader, 1994).

$$aA (g \rightarrow l) + bB (l) \rightarrow cC \qquad \text{or} \qquad A + b/aB \rightarrow c/aC \qquad (2)$$

where A = VOC, B = ClO_2, C = product, and a, b, and c are molar coefficients of the reaction. In a well mixed batch reactor the rate law for the reaction is,

$$-r = -\frac{1}{b}\frac{dB}{dt} = k_2 B^n A^m \qquad (3)$$

where, r is the reaction rate, k_2 is the rate constant and n and m are reaction orders with respect to each reactant. If the VOC is added to the mixture in excess of ClO_2, the rate law becomes

$$-\frac{dB}{dt} = k_1 B^n \tag{4}$$

$$k_1 = k_2 A^m \tag{5}$$

For a reaction first-order in B, Equation 4 can be solved for B and a plot of $\ln[B_0/B]$ versus time used to determine the pseudo-first-order rate constant, k_1, where B_0 is the initial concentration of the ClO_2. If the $\ln[Bo/B]$ versus time plot is a straight line, then the reaction can be considered first order. The reaction order with respect to A (*m*) can be determined from Equation 5 by plotting $\ln(k_1)$ versus $\ln(A)$, and for a straight line the slope is equal to *m* and the intercept equal to $\ln(k_2)$.

2.2.2.2 Batch method

In early experiments reactions were measured by injecting chlorine dioxide stock solutions into UV cells (10 mm, 4 ml total volume) containing the VOC of interest. The mixture was rapidly mixed via inversion of the closed cell and ClO_2 absorbance measured at 358 nm at 3-sec intervals. Reaction temperature was controlled by using a thermostated UV cell at 23-25°C and pH was controlled from 3.5 to 11 using buffer systems.

2.2.2.3 Stopped-flow method

To increase kinetic accuracy a stopped-flow device (Hi-Tech Scientific, Model SFA-20) was connected to the spectrophotometer (Beckman DU 650). Fresh reagent (ClO_2) and substrate (VOC) were loaded in individual syringes and rapidly pumped through a thermostated line with an in-line mixer, into and rapidly out of a flowcell (10 mm optical path length), typically in less than 8 msec, and then finally into a stopping syringe, with a minimum volume per reaction of 100 µl. An external water bath (GAC Corp., Precision) and pump was used to maintain a

constant temperature in the thermostated line of the stopped-flow device and temperature was monitored using a thermocouple (Omega Digital Thermometer, Type T thermocouple). The initial concentration ratio of substrate (VOC) to reagent (ClO_2) was maintained at least 5:1 to promote pseudo first order conditions. A minimum of 20 ClO_2 absorption data points were recorded during each run at 0.1 sec intervals, and at least two parallel kinetic runs were performed to determine a rate constant. Control experiments were performed without the VOC present at each temperature and pH in which stopped-flow experiments were performed to measure the background loss in absorbance due to decomposition of ClO_2.

2.2.3 Rendering process

Wet scrubber analysis was performed on a packed-bed, wet scrubber (ClO_2, 50 mg/L - 1 g/L) used to treat non-condensable gases from batch feather/blood hydrolyzers and continuous cookers. Removal efficiency analysis was performed on this first stage scrubber, which was sized to handle 33,994 m^3/h (1.9 m diameter, 3.5 m of packing). The scrubbing solution consisting of chlorine dioxide was passed across the packing at 814 L/min with approximately 90% recycle (i.e., 10% blow down). Scrubber analysis was performed as outlined in Kastner et al., (2002).

2.2.4 Simulation (mass transfer with chemical reactions)

The overall removal rate of the VOC in the scrubber was assumed to be a function of three resistances located in the gas film, liquid film, and bulk liquid (Levenspiel, 1999).

$$-r_A = \frac{1}{\dfrac{1}{k_{Ag}a} + \dfrac{H_A}{k_{Al}aE} + \dfrac{H_A}{kC_B f_l}} p_A$$

(6)

where $-r_A$ is overall rate of VOC removal (e.g., moles/s) per unit reactor volume, E is the enhancement factor due to chemical reaction defined as the ratio of the rate of VOC transfer with chemical reaction to the rate of transfer without reaction, H_A is the Henry's Law constant for the VOC, a is ratio of the gas-liquid interfacial area to reactor volume, k is the reaction rate constant for the VOC, k_{Ag} and k_{Al} are gas and liquid mass transfer coefficients for the VOC, C_B the concentration of the oxidizing agent, p_A the partial pressure of the VOC, and f_l the fraction of liquid volume in the reactor. The enhancement factor was calculated using the instantaneous enhancement factor (E_i) and Hatta number (M_H) as outlined in Levenspiel (1999). The Hatta number is defined as the ratio of the maximum VOC conversion in the liquid film to the maximum rate of mass transfer in the liquid film. E, E_i, and M_H all depend on the reaction order of the system. Juvekar and Sharma (1977) derived expressions for Ei and MH depending on the reaction order.

$$E_i = 1 + \frac{D_B}{D_A} \frac{B_o}{bA^*}$$

(7)

$$M_H = \frac{\sqrt{\frac{2}{m+1} D_A k_{mn} A^{*m-1} B^{o\,n}}}{k_{Al}}$$

(8)

Once the rate equation is defined it can be used in a differential mass balance equation over an absorber for both the liquid and gas phases to develop the reactor design equation. The general reactor design equations for gas-liquid reactions are the following:

$$\frac{dY_A}{dV_r} = \frac{-r_A a}{F_g} p_A = -\frac{\dfrac{1}{\dfrac{1}{k_{Ag}a} + \dfrac{H_A}{k_{Al}aE} + \dfrac{H_A}{kC_B f_l}}}{F_g} p_A \tag{9}$$

$$\frac{dX_B}{dY_A} = -\frac{F_g b}{F_l} \tag{10}$$

The equations above assume plug flow in both the liquid and gas, and isothermal conditions.

2.3 RESULTS AND DISCUSSION

2.3.1 ClO$_2$ kinetics

Rapid reaction rates are required for poorly water soluble compounds to be removed at high removal efficiencies in wet scrubbers. The chemical oxidizing agent, chlorine dioxide (ClO$_2$), although widely used in the rendering industry did not react with hexanal and 2-methylbutanal at pH 3.66 and 23-26°C. This is supported by the fact that absorbance monitored at 358 nm did not change when ClO$_2$ and these aldehydes were contacted, compared to the rapid change in absorbance for the reduced sulfur compounds (Fig. 2.1). The result that ClO$_2$ does not react with hexanal and 2-methylbutanal (and thus we assume 3-methylbutanal as well) indicates that the aldehydes are removed via mass transfer only. These results also compare favorably to reactions of ClO$_2$ with benzaldehyde, which has a reported rate constant less than 3 x 10^{-4} (L/mol-s at pH 8) with ClO$_2$ (Hoigne and Bader 1994).

2.3.2 Reaction order

As previously noted, experiments were designed such that the volatile organic compound (e.g., 2-methylbutanal) was in excess relative to ClO_2 and the rate law considered pseudo first order (Hoigne and Bader, 1994 & 1983). Under these conditions a plot of $\ln[Bo/B]$ versus time was used to determine the pseudo-first-order rate constant, k_1 (considered first-order, $n = 1$, if a straight line) and the reaction order with respect to A (m) determined by plotting $\ln(k_1)$ versus $\ln(A)$ with the slope (assuming a straight line) equal to m and the intercept equal to $\ln(k_2)$. Semi-log plots of absorbance versus time for ethanethiol were linear ($R^2 \geq 0.99$) indicating pseudo-first-order kinetics (data not shown). However, absorbance versus time plots for dimethyl disulfide (assuming first-order) were not linear ($R^2 < 0.95$), suggesting a different mechanism or reaction order (Fig. 2.2). Consequently, an alternative rate law was theorized for dimethyl disulfide (DMDS) – an overall third order reaction, second order in ClO_2 and first order in DMDS,

$$- r_B = -\frac{dB}{dt} = k_3 B^2 A^1 \tag{11}$$

where, $-r_B$ is the reaction rate and k_3 is the third-order rate constant. If DMDS or A is added to the mixture in excess of ClO_2, the rate law becomes second-order with respect to B or ClO_2.

$$-\frac{dB}{dt} = k_2 B^2 \tag{12}$$

$$k_2 = k_3 A^m \tag{13}$$

For a reaction second order in B, Equation 12 can be solved for B and a plot of $(1/B -$ $1/B_0)$ versus time and used to determine the pseudo-second-order rate constant, k_2, where B_0 is the initial ClO_2 concentration. If the plot is a straight line, then the reaction can be considered second order in ClO_2 (n = 2). A significant improvement in the goodness of fit to the kinetic data was obtained when assuming a pseudo-second order reaction for DMDS (Fig. 2.2).

The reaction of ethanethiol with ClO_2 was first-order in ClO_2 (or B), since a plot of $\ln(k_1)$ versus $\ln(B)$ yielded a straight line (Fig. 2.3) with the slope, m, never significantly deviating from 1 (0.93 ± 0.03). Consequently the overall reaction order for ethanethiol reacting with ClO_2 was determined to be second order, since $k_2 = k_1/B$ remained constant.

2.3.3 Temperature and pH dependence

Since reaction rates are a function of temperature and pH, these parameters were systematically altered to determine their effect on VOC oxidation. Regardless of the increase in temperature and pH, a significant increase in the reaction rate of hexanal and 2-methylbutanal with ClO_2 did not occur (data not shown), contrary to ethanethiol and dimethyl disulfide, which showed a significant increase in the reaction rate with ClO_2 as pH or temperature were increased (Fig. 2.4 and 2.5). These data suggest that a majority of the VOCs in rendering emissions, that is, aldehydes, do not react with ClO_2 and are only removed via absorption.

Rate constants for ClO_2 reacting with ethanethiol and dimethyl disulfide both increased with temperature (Fig. 2.4), however there was no measurable reaction with the aldehydes at higher temperatures. The reaction of ethanethiol appeared to follow the Arrhenius equation, but a semi-log plot of k_3 versus $1/T$ appeared to deviate from a straight line for dimethyl disulfide (Fig. 2.4). The activation energy for ethanethiol was found to be 13,000 cal/mol and the

frequency factor was 9.43×10^{10} L/mol/s ($R^2 = 0.997$), compared to an activation energy of 27,363 cal/mol and frequency factor of 2.285×10^{25} $L^2/mol^2/s$ ($R^2 = 0.76$) for dimethyl disulfide. Comparison of Fig. 2.4 and 2.5 indicates that pH had a more significant effect on the reaction rate, especially for ethanethiol. As noted in Fig. 2.5, the second order rate constant for ethanethiol increased exponentially with pH. Because the reaction rate was extremely fast above pH 5, it was difficult to obtain accurate kinetic data at higher pH values, and extrapolation was performed to estimate k_2 at higher pH values (see discussion). The second-order rate constant for ethanethiol was estimated as 4×10^4 and 4×10^6 (L/mol/s) for pH 6 and 8 respectively, similar to a value of 5×10^5 (L/mol/s) for 2-methyl-1 propane thiol at pH 8 (Hoigne and Bader, 1994).

Reaction rates were significantly larger for ethanethiol and dimethyl disulfide (DMDS), compared to the aldehydes and increased exponentially with pH. The exponential increase in the rate constant with pH indicates the dissociated form of ethanethiol reacts at a much higher rate with ClO_2. These results compare favorably to previously measured rate constants for ClO_2 reacting with 2-methyl-1-propanethiol (5×10^5 L/mol-s, pH 2-5.5) (Overcamp, 1999). The significantly different response of the rate constant for DMDS to an increase in pH (flat from pH 3.6 to 7, followed by an exponential increase from 7 to 10.6) and the fact that DMDS does not dissociate suggests a mechanism different from ethanethiol (and thiols in general). It is possible that a consecutive reaction occurs between DMDS (A) and ClO_2 (B) that results in a product from the first reaction that dissociates and reacts at a much higher rate with ClO_2 (i.e., A+B $\rightarrow$C, C+B$\rightarrow$ D).

2.3.4 Modeling

The kinetic data for ethanethiol oxidation was used to model gas absorption with chemical reaction for methanethiol. First the Hatta (M_H) number and E_i were calculated, assuming m = 1, according to:

$$M_H = \frac{\sqrt{D_A k_2 C_{Bo}}}{k_{Al}}$$

(14)

$$E_i = 1 + \frac{D_B C_{Bo} H_A}{b/a D_A p_{Ai}}$$

(15)

The liquid phase mass transfer coefficient was estimated using the correlation of Onda et al., (1959) which requires the liquid phase density, viscosity, diffusivity, and the total surface area of the packing. We also assumed that the kinetics measured for ethanethiol would be similar to methanethiol. Ethanethiol was chosen as the model compound because it was less volatile than methanethiol and a liquid at room temperature, and thus could be utilized in the batch kinetic studies. Additional assumptions were that b/a = b = 2 (Hoigne and Bader 1994) and the partial pressure of the VOC at the interface, p_{Ai}, equaled the partial pressure in the bulk gas phase, p_A (as an initial guess in evaluating equation 15).

Using the second order rate constant for ethanethiol reacting with ClO_2 a Hatta number of 1.8 was determined at a pH of 3.66 (C_B = 65 mg/L, T=35°C, P=1atm, C_g=4 ppmv). A Hatta number between 0.02 and 2 indicates that the reaction is slow enough to allow some of A (the VOC) to penetrate into the bulk liquid and react with B (ClO_2) (Levenspiel, 1999). However, a small increase in pH would raise the Hatta above 2, allowing for all of the reaction to occur in the liquid film. This suggested that the overall rate equation (Equation 6) could be modified to

exclude any reaction in the bulk liquid. Since k_2 and D_{Al} are not strong functions of temperature (over the temperature range expected in an industrial scrubber), the effect of pH on the Hatta number (M_H) was determined. In addition, since the instantaneous enhancement factor, E_i, was always five times greater than M_H, E was assumed equal to M_H, also indicating a pseudo first order reaction (Levenspiel, 1999). The Enhancement factor, E or M_H, increased significantly as the pH was slightly increased (Figure 2.6). The increase in E or M_H above 2 indicated that the reaction would take place at the gas-liquid interface or all within the liquid film and thus significantly increase the overall removal rate (Levenspiel, 1999).

Using experimental values for k_2 and $E = MH = \dfrac{\sqrt{D_A k_2 C_B}}{k_{Al}}$ the reactor design equation was solved numerically to determine the gas phase concentrations of the VOC (i.e., methanethiol) as a function of reactor height. Assuming dilute solutions and a pseudo first order reaction, the following changes were made to the design equations:

$$-\frac{dp_A}{dh} = \frac{S\pi(-r_A a)}{F_g} p_A = S\pi a \frac{\dfrac{1}{\dfrac{1}{k_{Ag}a} + \dfrac{H_A}{k_{Al}aE}}}{F_g} p_A \tag{16}$$

$$\frac{dC_B}{dp_A} = -\frac{bC_T}{\pi} \frac{F_g}{F_l} \tag{17}$$

Equation 17 was assumed to apply over a differential change in reactor height and solved to predict the consumption of ClO_2 over the column. Pseudo first order kinetics was verified using equation 18; e.g., at an inlet ClO_2 concentration of 1 g/L a 1.5% reduction in ClO_2 is predicted ($p_A$in=0.405 Pa or 4.05 ppmv, a 95% conversion, and see Table 2.1 for other inputs).

$$C_B = C_{Bo} - \frac{bC_T}{\pi}\frac{F_g}{F_l}\left(p_{Ao} - p_A\right)$$

Using the model for mass transfer with chemical reaction, parameters based on vendor data, and estimates from the literature (Table 2.1), the predicted packing height required for a range of methanethiol conversions as a function of the reaction rate constant was calculated and compared to field scale data. The model predicts a significant increase in methanethiol conversion efficiency (using kinetics for ethanethiol) as the pH and thus overall reaction rate is increased (Figure 2.7). However, the model clearly under-predicts methanethiol conversion efficiency at the measured pH values of the scrubbing solution and reported operational packing height of the scrubber (Figure 2.7).

It is unclear as to why the kinetic model did not predict the field scale results. One possibility was that the kinetics of ClO_2 oxidation with methanethiol is faster than for ethanethiol. However, the pKa for methanethiol is 10.7, which is not significantly different from ethanethiol (pKa = 10.6) (Dean, 1992), indicating the effect of pH on the rate constant would be similar. Steric effects only accounted for a 16% reduction in the acid catalyzed esterification of CH_3COOH versus CH_3CH_2COOH (Conners, 1990), and thus are unlikely to account for the apparently large difference in reaction rates between the field scale scrubber and the kinetic model. Order of magnitude changes in parameters obtained from correlations or the literature (i.e., k_l, k_g, D_{Al}, b=1) and process inputs (F_g, F_l) couldn't account for the differences as well. Other possibilities were that scrubbing solution pH was actually higher than that recorded using in-line probes or residual chlorine was produced via the on-site ClO_2 generator which would react at a much higher reaction rate (Kastner and Das, 2002). The opposite appears to be true for the aldehyde fraction. Kinetic data coupled with the removal efficiency data and simulation

studies indicate that low removal efficiencies for the aldehydes and alkanes are due to lack of a reaction with ClO_2.

2.4 CONCLUSION

Batch kinetic analysis can be used to rapidly screen oxidizing agents to determine if they oxidize and remove air pollutants in rendering emissions and can also be used to rapidly determine optimum operating conditions, such as pH and oxidizing agent concentration. Moreover, the kinetic data can be used in models to predict trends in removal efficiency in industrial scale scrubbers.

The kinetic analysis also indicates that chlorine dioxide does not react with hexanal and 2-methylbutanal (and presumably the entire aldehyhde fraction) over a wide range of pH and temperatures, which constitutes a major fraction of VOC emissions. Contrary to the aldehydes, ethanethiol (a model compound for methanethiol) and dimethyl disulfide rapidly reacted with ClO_2. Moreover, an increase in pH from 3.6 to 5.05 exponentially increased the reaction rate of ethanethiol and significantly increased the reaction rate of dimethyl disulfide if increased to pH 9 (these results should also apply to methanethiol). Thus, a small increase in pH could significantly improve wet scrubber operations for removal of odor causing compounds. Further research is required to improve wet scrubber models using kinetic analysis, including a more accurate model for disulfides and incorporation of multiple VOCs reaction kinetics with the oxidizing agent in the scrubbing solution. The model could be used to optimize wet scrubber operations using ClO_2 or other oxidizing agents provided kinetic data are available.

Notation

a	gas-liquid interfacial area per unit volume reactor (m^2/m^3)
a_w	area of packing wetted by the flowing liquid per unit volume of packed bed.
A	absorption factor defined as (L / mG)
A^m	VOC liquid phase concentration (mol/m^3)
B_0	ClO_2 liquid phase concentration (mol/m^3)
C_B	ClO_2 liquid phase concentration (mol/m^3)
C_{Bo}	ClO_2 liquid phase concentration (mol/m^3)
C_T	Total liquid phase concentration (mol/m^3)
D_{Al}, D_A	Diffusivity of the VOC in the liquid phase (m^2/s)
D_B	Diffusivity of ClO_2 or ozone in the liquid phase (m^2/s)
E	Enhancement factor
E_i	Instantaneous enhancement factor
f_l	ratio of liquid volume to reactor volume
F_g	molar flow rate the inerts in the gas phase (mol/s)
F_l	molar flow rate of the inerts in the liquid phase (mol/s)
g	gas phase
G	volumetric flow rate of the gas stream
G_m	superficial mass velocity of gas.
h	Height of wet scrubber (m)
H_A	Henry's Law contant, (m^3-Pa/mol-s)
k_{Ag}	gas phase mass transfer coefficient (mol/m^2-s-Pa)
k_{Al}	liquid phase mass transfer coefficient (m/s)
k'_{Al}	liquid phase mass transfer coefficient with chemical reaction (m/s)
k_1	Pseudo first order rate constant (1/s)
k_2	Overall second order rate constant (l/mol/s)
k_3	Overall third order rate constant ($l^2/mol^2/s^2$)
K_G	Overall mass transfer coefficient for the gas phase.
l	liquid phase
L	volumetric flow rate of the liquid stream
M_H	Hatta number

p_A	Partial pressure of VOC at any point in the wet scrubber (Pa)
p_{Ai}	Partial pressure of the VOC at the liquid-gas interface (Pa)
p_{Ao}	Partial pressure of VOC at the inlet of the wet scrubber (Pa)
m	slope of the equilibrium curve (equal to the Henry's law constant for dilute solutions).
r_A	overall rate of VOC removal (e.g., moles/s) per unit reactor volume
y_1	mole fraction of the entering gas.
y_2	mole fraction of the exiting gas.
Y_A	mole fraction of the VOC based inerts in the gas phase
x_1	mole fraction of the exiting liquid.
x_2	mole fraction of the entering liquid.
X_B	mole fraction of ClO_2 based on inerts in the liquid phase
ρ_G	gas phase density
S	Cross sectional area of wet scrubber (m^2)
π	Sum of the partial pressure of the components in the gas phase

REFERENCES

Barnes, R. D., MacLeod, A. J., 1982. Analysis of the composition of the volatile malodorous emissions from six animal rendering factories. *Analyst*, 10, 711-715.

Brewer, M. S., Vega, J. D., Perkins, E.G., 1999. Volatile compounds and sensory characteristics of frying fats. *Journal of Food Lipids*, 6, 47-61.

Conners, K. A., 1990. *Chemical Kinetics: The Study of Reaction Rates in Solution*. New York: VCH Publishers.

Dean, J. A., 1992. *Lange's Handbook of Chemistry*, 14th Edition. New York: McGraw-Hill.

Greenberg, A. E., Clesceri, L. S., and Eaton, A. D., 1992. *Standard methods for the examination of water and wastewater*. Washington: American Public Health Association.

Hoigne, J., Bader, H., 1994. Kinetics of Reactions of Chlorine Dioxide (OClO) in Water-I. Rate Constants for Inorganic and Organic Compounds; *Wat. Res*., 28, 45-55.

Hoigne, J., Bader, H., 1983. Rate Constants of Reactions of Ozone with Organic and Inorganic Compounds in Water-I: Non-Dissociating Organic Compounds. *Wat. Res*., 17, 173-183.

Hrudey, S. E., Gac, A., Daignault, S. A., 1988. Potent odor-causing chemicals arising from drinking water disinfection. *Water Sci. Technol*, 20, 55-61.

Juvekar, V., Sharma, M. M., 1977. Some aspects of process design of gas-liquid reactors. *Trans. Instn. Chem. Engrs*, 55, 72.

Kastner, J. K., Das, K. C., 2002. Wet Scrubber Analysis of Volatile Organic Compound Removal in the Rendering Industry. *J. Air & Waste Manage. Assoc.*, 52, 459-469.

Levenspiel, O., 1999. *Chemical Reaction Engineering*. New York: John Wiley & Sons.

Onda et al., 1959. *Am. Inst. Chem*. Eng. J., 5, 235.

Overcamp, T. J., 1999. Modeling Oxidizing Scrubbers for Odor Control. *Environ. Sci. Technol.*, 33, 155-156.

Prokop, W. H., 1974. Wet Scrubbing of inedible rendering plant odors. *In Proceedings of AWMA Specialty Conference on Odor Control Technology I, Air & Waste Management Assoc.*, Pittsburgh PA, 132-150.

Prokop, W. H., 1985. Rendering Systems for Processing Animal By-Product Material. *JAOCS*, 62, 805-811.

Prokop, W. H., 1991. Control Methods for Treating Odors Emissions from Inedible Render Plants. *Proceedings of Air & Waste Management Assoc., 84th Annual Meeting*, Vancouver, BC. Article 91-146.8., 1-16.

Tenney, J., Crump, B., Ernst, W., Gravitt, A., Isaac, T., 1997. Froth Reactor for Small-Scale Generation of Chlorine Dioxide. *AIChE Journal*, 43, 2148-2152.

Table 2.1 Model inputs for wet scrubber with chemical reaction.

Parameter	Input and Units		Description
a	85	m^2/m^3	Total packing surface area
b	2		Moles of ClO2 consumed per mole of VOC consumed
C_{Bo}	15	mol/m^3	Inlet ClO2 concentration
C_T	55,317	mol/m^3	Total concentration of liquid phase
D_{Al}	1.2 x 10-9	m^2/s	Diffusivity of the VOC in water at 35°C
f_l	0.1		Ratio of liquid volume to reactor volume
F_g	390.74	mol/s	Gas flow rate
F_l	771.6	mol/s	Liquid flow rate
H_A	376	m^3-Pa/mol-s	Henrys Law constant, 35°C
k_{Ag}	1.89 x 10-5	mol/m^2-s-Pa	Gas phase mass transfer coefficient
k_{Al}	7.83 x 10-4	m/s	Liquid phase mass transfer coefficient
k_2	0.0025 – 6 x 106	m^3/mol-s	Second order rate constant
π	101,324.6	Pa	Sum of partial pressures
p_{Ao}	0.405	Pa	Inlet VOC partial pressure
T	35	°C	Temperature of liquid scrubbing solution
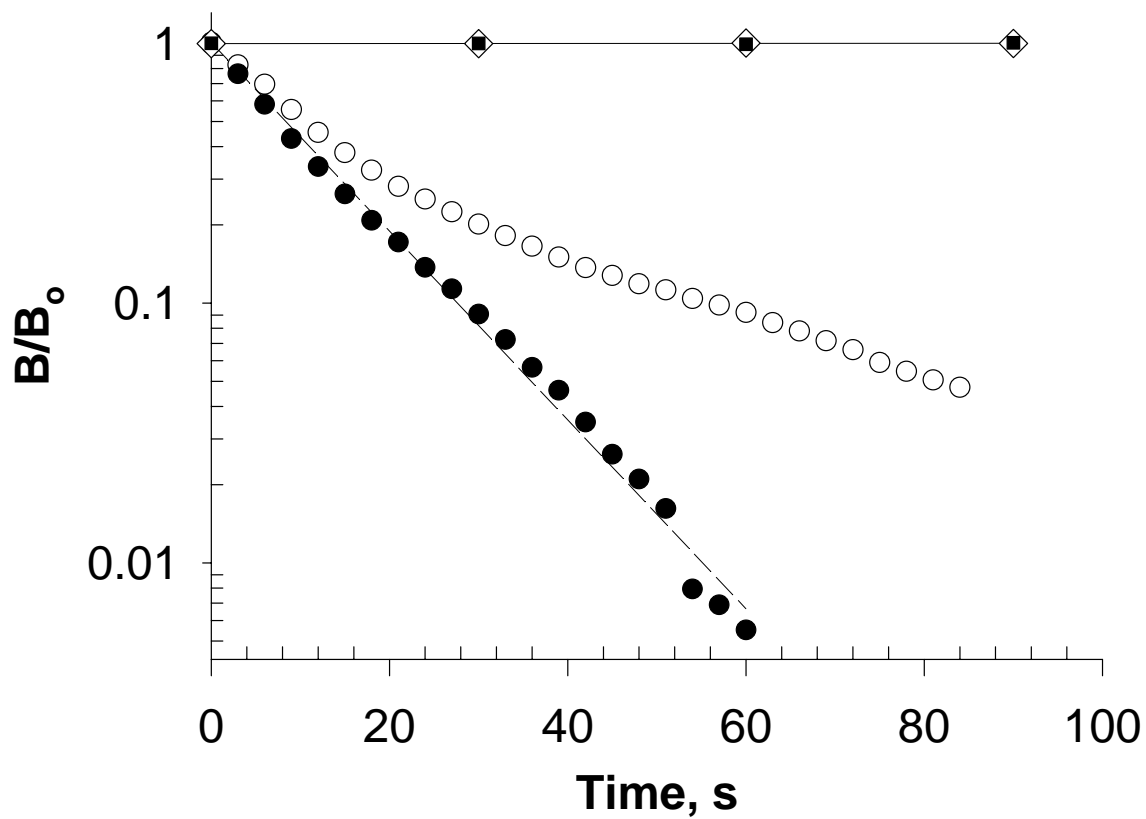
Fig. 2.1 Batch reaction of ClO_2 (98 mg/L) with hexanal ($\diamond$) and 2-methylbutanal ($\blacksquare$), and the reduced sulfur compounds ethanethiol ($\bigcirc$) and dimethyl disulfide ($\bullet$) at pH 3.36. The concentration of the volatile organic compound was 477 mg/L to maintain a 4:1 ratio of VOC to ClO_2 and pseudo- first-order conditions.
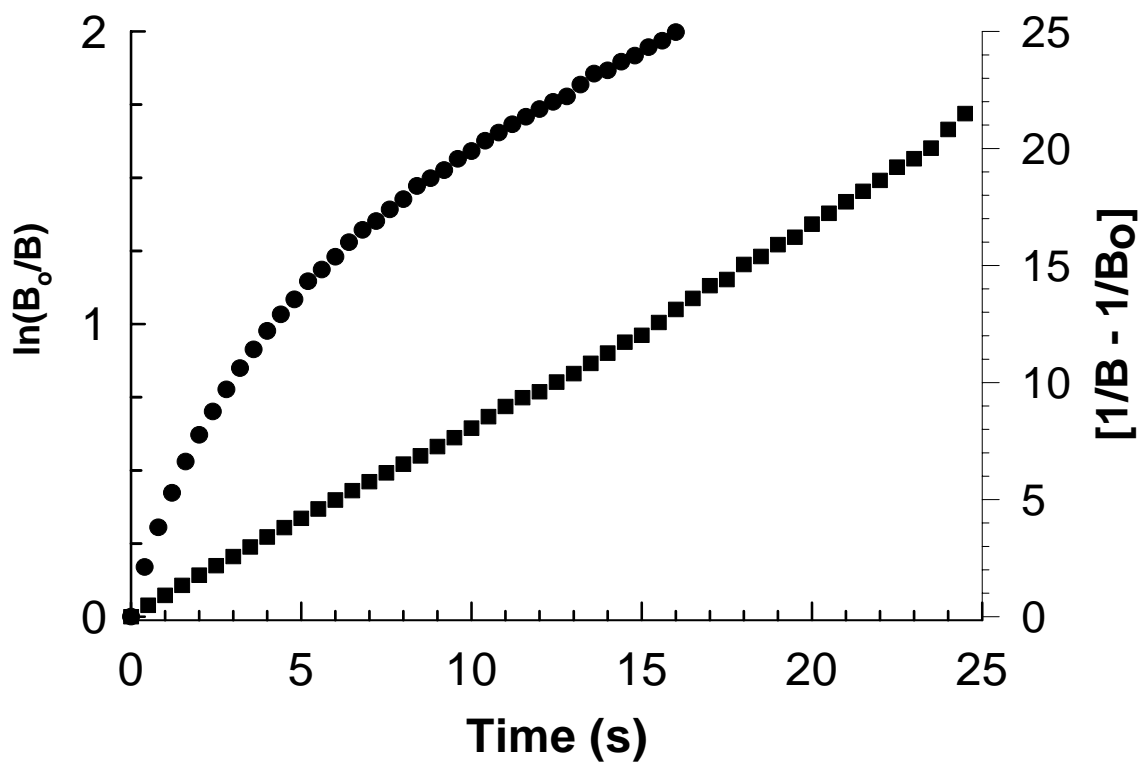
Fig. 2.2 Change in absorbance for the reaction of ClO2 with dimethyl disulfide (DMDS) assuming pseudo first order kinetics (second order overall), (●) and pseudo second order (third order overall), (■).
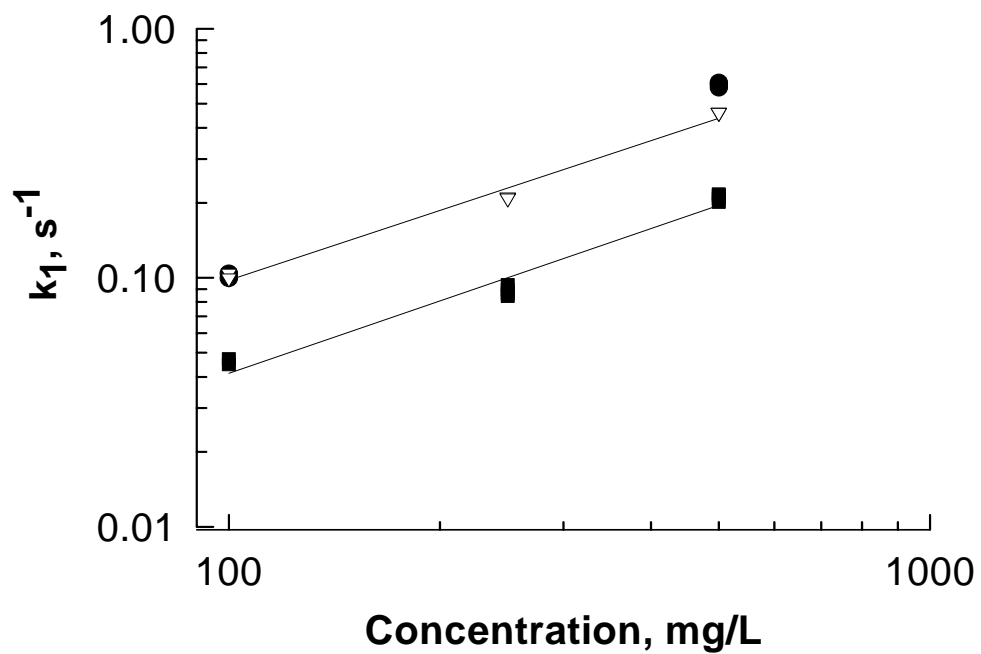
Fig. 2.3   Plot of k1 versus substrate concentration for ethanethiol reacting with ClO_2 (20-50 mg/L) at temperatures of 22-24°C (■), 35-37°C (▽), and 40°C (●), and a pH of 3.58. The concentration of ethanethiol ranged between 100-500 mg/L to maintain a 5:1 ratio of ethanethiol to ClO_2.

26
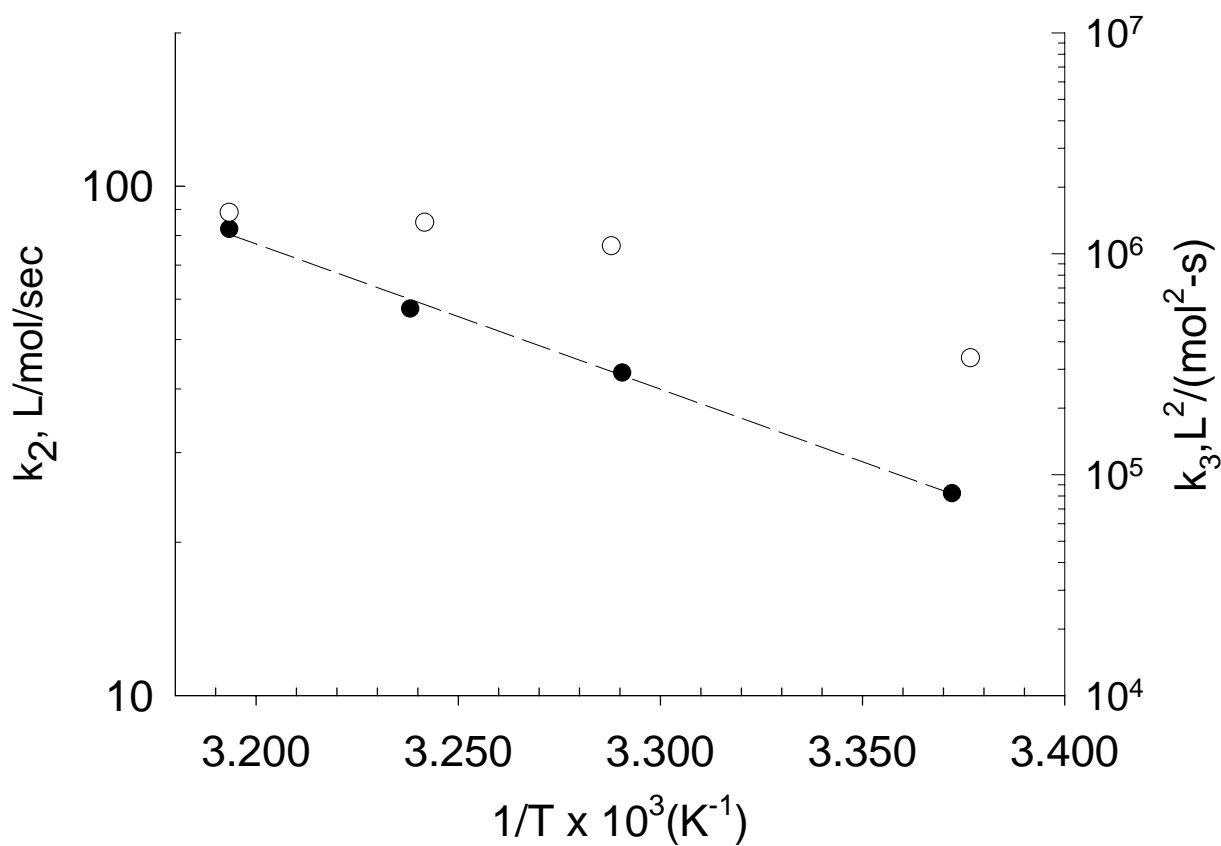
Fig. 2.4 Arrhenius plots for the overall rate constants of ClO_2 reacting with ethanethiol (●) and dimethyl disulfide (○) at pH 3.6 (hexanal and 2-methyl butanal did not react with ClO_2 at increasing temperatures).
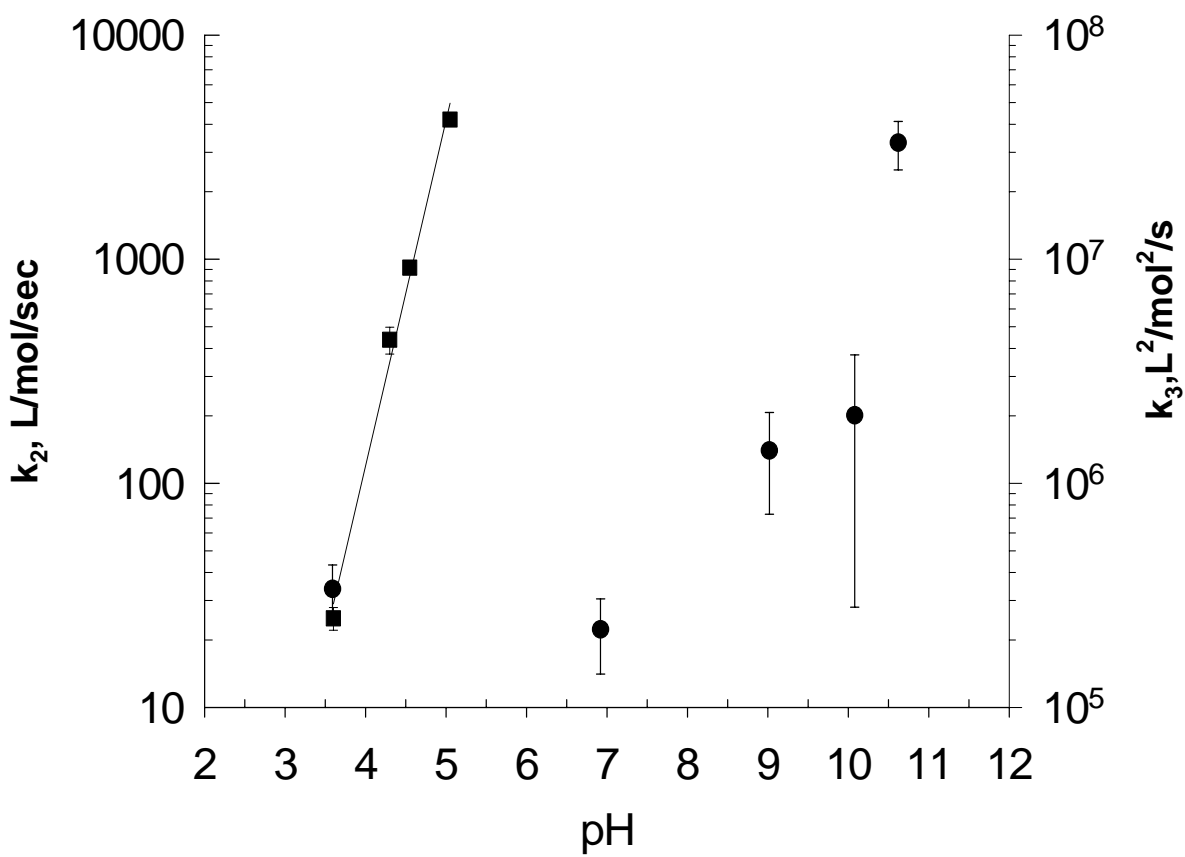
Fig. 2.5   Effect of pH on the second and third order rate constant of ClO_2 reacting with ethanethiol (■) and DMDS (●) at a temperature ranging between 23-25°C.
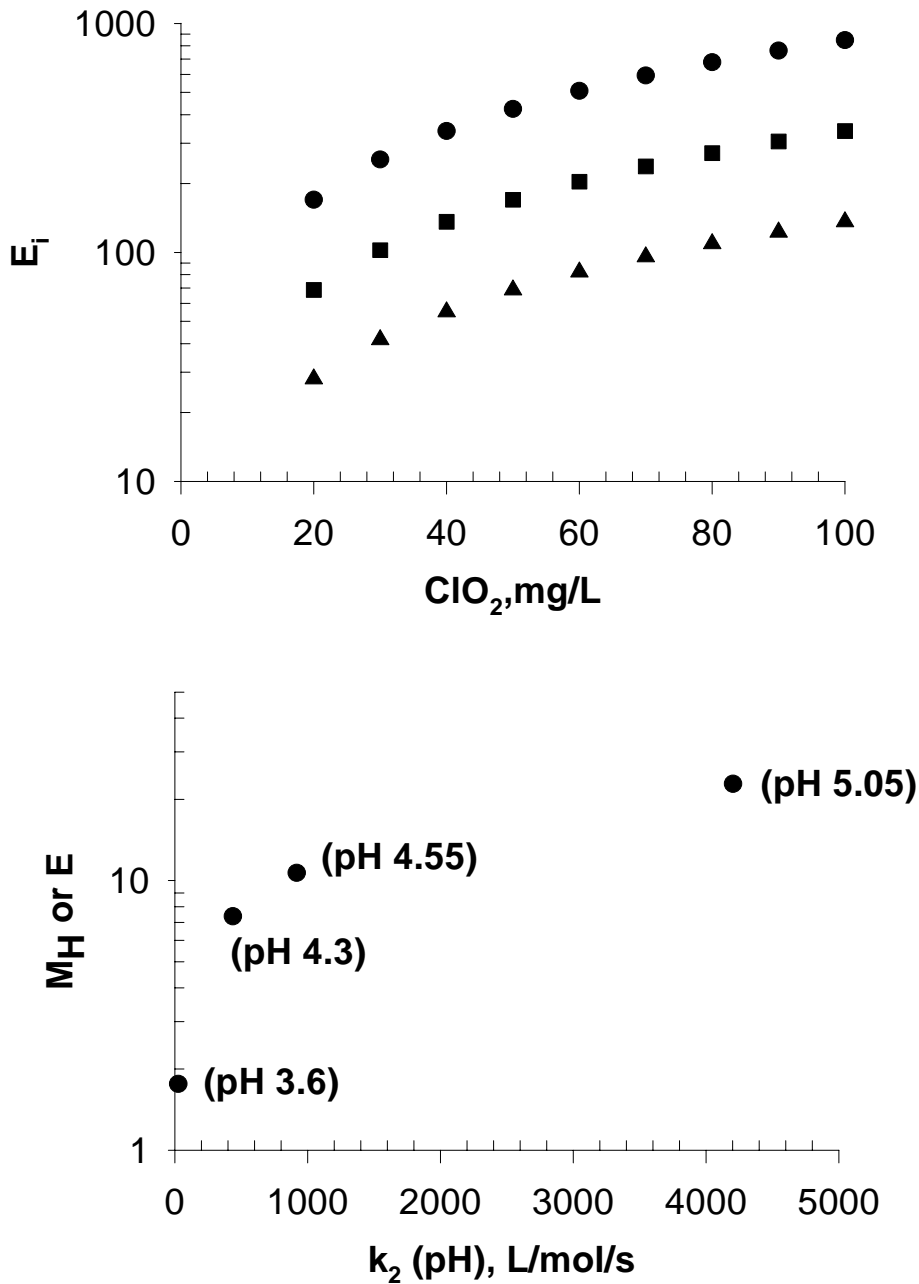
Figure 2.6   The effect of ClO_2 concentration (A) at three different inlet methanethiol concentrations, 4 (●), 10 (■), and 25 (▲) ppmv on E_i and the effect of pH on the Enhancement factor, E, for methanethiol (B). All parameters in the model were calculated at a temperature of 35°C and the rate constant measured for ethanethiol was assumed valid for methanethiol.
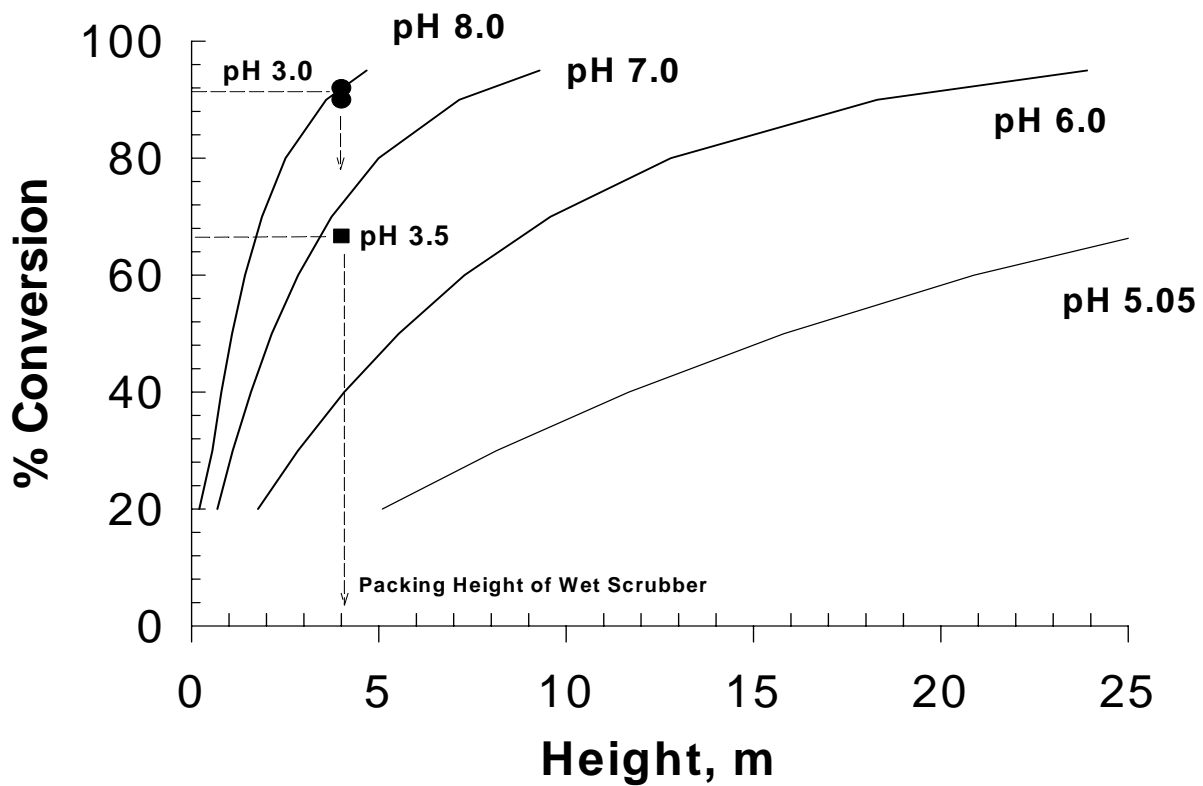
Figure 2.7 The effect of pH (i.e., reaction rate constant) on the packing height required for different methanethiol removal efficiencies predicted via the model versus experimental data (pH 3.0, ●; pH 3.5, ■) measured in an industrial scale scrubber (4 m packing height) using ClO_2. All parameters were calculated using a temperature of 35°C and an inlet ClO_2 concentration of 1 g/L, and experimental conversion efficiencies were based on a detection limit of 0.3 ppmv (Kastner and Das, 2002).

CHAPTER 3

MODELING REACTION KINETICS OF CHLORINE DIOXIDE AND VOLATILE

ORGANIC COMPOUNDS WITH ARTIFICIAL NEURAL NETWORKS[1]

_____

To be submitted to *Computational Biology and Chemistry*.

Abstract

Wet scrubbers are primarily used in the rendering industry to remove odorous harmful organic compounds. Chlorine dioxide is the major oxidant used in wet scrubbers to oxidize those volatile organic compounds (VOCs). Reaction kinetic data of chlorine dioxide and VOCs are important to wet scrubber design and optimization, but they are lacking. Deriving reaction kinetic equations through the study of their reaction mechanisms is difficult because the reaction of chlorine dioxide and VOCs is complicated and involves multiple steps and several intermediate products. Therefore, artificial neural networks are applied here to model the reaction kinetics without the prior knowledge of reaction mechanism. A k-fold cross validation approach was adopted to partition the data and evaluate model performance. Through the selection of suitable network architectures and network parameter optimization, a standard three-layer feed-forward network with back-propagation learning algorithm was developed to predict the initial reaction rate of chlorine dioxide with ethanethiol and dimethyl disulfide. For ethanethiol, the average mean square error (MSE), mean absolute error (MAE), and R squared value the model produced on the three production data sets (pH 3.73, 3.92, 4.01) are 17.807, 3.471, and 0.9279 respectively. For DMDS, the average MSE, MAE, and R squared value the model produced on the four production data sets (pH 5.26, 6.92, 7.62, and 9.02) are 4.437, 1.589, and 0.8566, respectively. A final model can be developed by using all the available data patterns as training data without a testing data set. The final model then can be used to predict the initial ClO_2 reaction rates with ethanethiol or DMDS for the design and optimization of wet scrubbers.

Keywords: artificial neural network, chlorine dioxide, volatile organic compounds, kinetics, modeling

3.1 INTRODUCTION

Poultry rendering operations convert organic wastes (feathers, offals, dead birds, blood, and hatchery byproducts) to products such as feed additives and fertilizer. The non-condensable gases produced during this process contain a wide range of volatile organic compounds (VOCs) that are typically passed through wet scrubbers units (Fig. 3.1) for air pollution control. Major VOCs identified in rendering emissions include dimethyl disulfide (DMDS), methanethiol, octane, hexanal, 2-methylbutanal, 3-methylbutanal, and 2-methylpropanal (Kastner and Das, 2002). The mechanism of VOC removal through wet scrubbers involves mass transfer and chemical oxidation. Chlorine dioxide is usually used as the oxidant in wet scrubbers. Thus, the reaction rate of chlorine dioxide and VOCs is one of the major factors that determine wet scrubber removal efficiency. Unfortunately, kinetic data of the reaction of chlorine dioxide and VOCs generated in the rendering industry are lacking, so the design and optimization of wet scrubbers are limited (Kastner et al., 2003).

With the resurgence of artificial neural networks (ANNs) in the mid-1980s (Russell and Norvig, 1995; Smith, 1993), ANNs have been applied in a wide variety of domains. The first well-known application of ANNs in chemistry and chemical engineering occurred in the late 1980s (Bulsari, 1995). ANNs have become a powerful and popular tool in chemistry and chemical engineering (Gasteiger and Zupan, 1993; Bulsari, 1995; Zupan and Gasteiger, 1999). Compared to traditional statistical methods such as multiple linear regression, principle component analysis, and principle component regression, ANNs have the advantages of nonlinear mapping, no prior knowledge requirement, and robustness to noisy data.

ANN research was initially motivated by the observation that biological learning systems are built of very complex webs of interconnected neurons. ANNs provide a general, practical

method for learning real-valued, discrete-valued, and vector-valued functions from examples. Learning algorithms such as back-propagation use gradient descent to adjust network weights to best fit a training set of input-output pairs (Mitchell, 1997). Because of its black-box characteristic, ANNs have been used in chemical reaction kinetic modeling by many researchers in recent years (Psichogios and Ungar, 1992; Blanco et al., 1995; Galvan et al., 1996; Bryjak et al., 2000; Safavi et al., 2001).

In this research, we will study the reaction kinetics of chlorine dioxide with two VOCs: ethanethiol and DMDS. In theory, reaction rates can be calculated from reaction rate equations. But it is difficult to derive these kinetic equations from their reactions, because oxidations of disulfides and thiols involve many steps and several intermediate products. The final oxidation product of disulfide is sulfonic acid. Figure 3.2 shows possible reaction steps and intermediates. Oxidation of thiol proceeds stepwise, producing disulfide initially, and finally sulfonic acid (Oae, 1977). Besides reactant concentrations, major factors that affect the reaction rate of the oxidation process include pH, temperature, and time. The relationships among the variables affecting the reaction rate, called the rate law, in many cases are non-linear. Also it is difficult to develop one rate law equation that adequately predicts the reaction rate as a function of these important variables.

The goal of this research was to use ANNs to model the reaction of chlorine dioxide and two VOCs (ethanethiol and DMDS) for subsequent use in designing wet scrubbers. The developed model would predict the initial reaction rate of chlorine dioxide with the VOCs based on inputs of initial concentrations of chlorine dioxide and VOCs, temperature, and pH. The objectives of this study were to:

1. Collect kinetic data on the reaction of chlorine dioxide and ethanethiol using a UV-VIS spectrophotometer and a stopped-flow device;

2. Collect kinetic data of the reaction of chlorine dioxide and DMDS using a similar approach;

3. Calculate the initial reaction rates from the collected experimental data and partition data sets for model development and model evaluation.

4. Develop ANN models for the reactions of chlorine dioxide and the VOCs and evaluate the performance of the models.

3.2 MATERIALS AND METHODS

3.2.1 Chemicals

All chemicals used in the study were of reagent grade. Ethanethiol was obtained from Aldrich, and DMDS was obtained from Acros Organics. Chlorine dioxide was prepared in an SVP-Pure^{TM} Chlorine Dioxide Generator (EKA Chemicals Inc.). The solution, about 2.2 g/L, is stored in dark bottles at 4°C up to 4 months. The maximum absorbance wavelength of ClO_2 checked by wavelength scanning was 358 nm and its molar absorptivity was calculated to be 1195 $M^{-1}cm^{-1}$. Chlorine dioxide concentrations were confirmed using the standard iodometric method (Greenberg et al., 1992).

3.2.2 Instruments

The oxidation of DMDS and ethanethiol are fast reactions, therefore a stopped-flow device (Hi-Tech Scientific, Model SFA-20) was connected to a UV-VIS spectrophotometer (Beckman DU 650). Fresh reagent (ClO_2) and substrate (VOC) were loaded in individual syringes and rapidly pumped through a thermostated line with an in-line mixer into and out of a

flow cell (10mm optical path length), typically in less than 8 milliseconds. The mixture then flowed into a stopping syringe with a minimum volume per reaction of 100 µL. An external water bath (GAC Corp.) with a pump (Precision) was used to maintain constant temperatures for the stopped-flow device.

3.2.3 Data acquisition

The initial concentration ratio of VOC to ClO_2 was equal to or larger than 5 to satisfy pseudo-first order conditions (Steinfeld, Francisco, and Hase, 1999). A minimum of 20 ClO_2 absorption data points was recorded during each run and the minimum data recording interval was 0.1 second. Most runs had a parallel replicate experiment, and some had three replicates. The initial reaction rate of chlorine dioxide was calculated by the method of numerical forward differencing based on the experimental data. The generation of one observation (or data pattern) usually required more than two hours including chemical solution preparation, instrument operation, and data processing. Therefore, the number of data patterns for ANN model development and evaluation are limited.

3.2.4 Neural network model development and evaluation

NeuroShell 2.0 (Ward System Group) was used to develop the ANN models. Separate models were developed for ethanethiol and DMDS. The four inputs to the ANN were VOC initial concentration, ClO_2 initial concentration, pH, and temperature. Imported data were scaled by the software. The ANN output was the initial consumption rate of ClO_2. All data were partitioned into model development and model evaluation sets. The model development data set was further partitioned into training data set and testing data set. The training data set was used to adjust ANN weights. The testing data set was fed forward through the ANN one time only to determine when to stop training and to save weights. Here the model evaluation data set is

referred to as the production data set. After extracting training, testing, and production data sets, users can select from several ANN architectures. ANN parameters such as initial connection weights, learning rate, momentum, and stop training criteria can be set manually. In our study, training was stopped and weights were saved automatically when the network produced minimum error on the testing data set. Network performance was evaluated on production data sets by statistical criteria of R squared, mean squared error (MSE), and mean absolute error (MAE). R squared is the coefficient of multiple determination, which is a statistical indicator usually applied to multiple regression analysis. The higher R squared value, the better fit of the model. MSE is the mean of the square of the actual value minus the predicted value over all patterns in the production data set. The unit of MSE here is $(mg\ L^{-1}\ s^{-1})^2$. MAE is the mean over all patterns of the absolute value of the actual minus the predicted, and its unit is $mg\ L^{-1}\ s^{-1}$.

3.3 RESULTS AND DISCUSSION

3.3.1 Model development for ethanethiol

3.3.1.1 Data partition

The experimental data set for the modeling of the reaction of chlorine dioxide and ethanethiol consisted of 89 data patterns (including replicates) were used to build and evaluate ANN models. Through the initial experiments and model development we found that of the four inputs, pH is the most important factor that affects the initial consumption rates of chlorine dioxide. Therefore we partitioned the data such that pH values used in the production data set were not used in model development (training and testing). Other input values in production sets may or may not been used in training and testing sets. After extracting the production data, 25% of the remaining data was randomly drawn to be the testing data set and the data left were used

as the training set. Value ranges of inputs and the numbers of patterns in each pH group are listed in Table 3.1. The only output is the initial reaction rate of chlorine dioxide.

For small data sets, usually k-fold cross-validation approach is recommended, in which cross validation is performed k different times, each time using a different partitioning of the data into model development and model validation sets, and the results are then averaged (Mitchell, 1997). In our modeling, in order to efficiently use available data as well as accurately evaluate the performance of ANN models, 5-fold cross validation strategy was used here. During each data partition, one group of pH data was held as the production data set and was not used in training and testing. Seven pH levels were observed in the experimental data: 3.58, 3.61, 3.73, 3.92, 4.01, 4.21, and 4.55. We grouped pH 3.58 and 3.61 together because these two buffers have very close pH values. When the pH reached 4.21, the reaction of chlorine dioxide and ethanethiol was very fast, but the instrument was not fast enough to record the very initial stage of reaction, so the data contain considerable noise. Also for the pH of 4.55, there are only seven patterns, so we grouped data at pH 4.21 and 4.55 into one set. Thus, we created five pH groups: 3.58 & 3.61, 3.73, 3.92, 4.01, and 4.21 & 4.55. Each of these pH groups was used once in production with the rest of the data in model development.

3.3.1.2 Network architecture selection

ANN models were initially developed with several ANN architectures such as the standard back-propagation nets and Ward nets. After optimization of network parameters, which include hidden layers, hidden nodes, activation functions, initial weights, learning rates, and momentums, a three-layer standard back-propagation ANN had the highest accuracy (smallest prediction error) on the five production data sets. Activation functions in each layer are shown in Fig. 3.3. The ANN was used for all subsequent model development.

3.3.1.3 Network parameter optimization

Each MSE, MAE, and R squared value shown from Table 3.2 to Table 3.4 were the average value on the five production data sets (as mentioned in the data partition section). For the standard ANN with one hidden layer (initial weights 0.1, learning rate 0.1, and momentum 0.1), results in Table 3.2 shows that three hidden nodes produced the smallest MSE and MAE, and the highest R squared. The number of hidden nodes had a greater effect on the model accuracy. The ANN with too many hidden nodes is easily to overfit data, while those with only a few nodes are not powerful enough to capture the relationships among inputs and outputs.

The effect of different initial weights under fixed learning rate and momentum (both 0.1) on the three-hidden node ANN was compared in Table 3.3. Small initial weights are usually recommended because it makes the output locate in the sensitive region of the logistic function (Mitchell 1997; Smith 1993). Large initial weights cause long training times and are more easily to overfit data. Here, the model prediction accuracy was not so sensitive to the initial weight settings. An iterative search for the optimum learning rate and momentum (initial weights 0.1) was done in Table 3.4. A suitable learning rate and momentum can prevent the network from being trapped in local minimum error surface. The best learning rate and momentum were 0.l respectively.

3.3.1.3 Modeling

The final ANN model is a standard three-layer back-propagation network (3 nodes in the hidden layer) with the following parameter settings: 0.1 initial weights, 0.1 learning rate and 0.1 momentum. Modeling statistics on the five production data sets are listed in Table 3.5. The model made the prediction at the first production set (pH = 3.58 & 3.61) by extrapolation at the low pH boundary, therefore, the R squared value is very low. ANNs are not generally used in

extrapolations outside the range of input values. For the production data set at 4.21 and 4.55, the R squared value is also low. There are two reasons. First, this pH group is located at the high pH boundary, so the network predicted reaction rates by extrapolation. Another reason causing the degradation is that the reaction of ethanethiol and chlorine dioxide above pH = 4.21 is so fast that the spectrophotometer cannot capture the changes of chlorine dioxide absorption at the beginning stage of the reaction. So, data above pH = 4.21 are noisy. The results for the other three production data sets (pH 3.73, 3.92, 4.01) were averaged yielding an average R squared value of 0.9279, an average MSE of 17.807, and an average MAE of 3.471.

Fig. 3.4 shows the prediction of the reaction rates for the production data set with a pH of 3.73. This is the best prediction of the three production data sets, which had the lowest error and the highest R squared value. A linear regression line (y = 1.009x – 1.8362) was fit to the predicted versus observed reaction rates and is shown along the 1:1 line. It indicates that the model has a slight tendency to under predict the reaction rate. Fig. 3.5 is the prediction of reaction rates for the production data set with a pH of 3.92, which has a slightly higher MSE and MAE, a lower R squared value than the predictions of pH of 3.73 and 4.01. The linear regression line (y = 0.9822x – 3.6636) also shows the ANN tended to consistently under predict the reaction rate. Fig. 3.6 is the prediction of reaction rates at pH = 4.01. The linear regression line (y = 0.76942x + 7.4952) shows that the ANN tended to over predict reaction rates lower than 35 mg $L^{-1} s^{-1}$, and to under predict reaction rates when they are above 35 mg $L^{-1} s^{-1}$.

After the model development and cross evaluation, a final model can be developed in this way for the future prediction (Mitchell, 1997): all the 89 patterns are used for training the three-layer standard back-propagation ANN with the optimal parameter settings and there is no testing data set. Stop training when the learning epoch is equal to the average value of the three learning

epochs in the model development and evaluation using the three production data sets (pH 3.73, 3.92, 4.01).

As an example, the 89 patterns were randomly partitioned with approximately one third being placed in model evaluation (29 patterns). The remaining 60 patterns were then used as model development. To avoid the situation that one pattern is in the training set and its replicate is in the production set, we manually examined each pattern in the production set. If we find two parallel patterns are separated, then put them together back in the training data set. In order to use all possible patterns in training, no testing data set was used in this example. Based on the results of prior model development, the training was stopped when the learning reached 595 epochs. After applying the ANN on the production set, the R squared was 0.9320. MAE and MSE were 3.903 and 25.291 respectively. Fig. 3.7 shows the predicted ClO_2 initial reaction rates versus the observed values. A linear regression line ($y = 0.8819x - 0.3856$) was fit to the predicted versus observed reaction rates. It indicates that the model has a slight tendency to under predict the reaction rates. Compared to the previous average result on the three production sets (pH 3.73, 3.92, and 4.01), the general model has a higher R squared value, a slightly higher MAE and MSE.

Fig. 3.8 shows that pH had a more significant effect than temperature on the initial reaction rate of chlorine dioxide in the reaction with ethanethiol. In (a), the initial concentrations of ethanethiol and ClO_2 were low (175 mg/L and 20 mg/L), while in (b), they were higher (375 mg/L and 40 mg/L). All the reaction rates were generated by the model using the same approach described above. The only difference was that all the 89 patterns here were used in model development. The production data set was generated manually.

3.3.2 Model development for DMDS

3.3.2.1 Data partition

For the reaction of DMDS and chlorine dioxide, a total of 149 data patterns (including replicates) were generated with the experiments which were used to develop and evaluate ANN models. The k-fold cross validation, here 6-fold, data partition strategy was used. All the pHs were divided into six groups as we had done for ethanethiol: 3.58 & 3.61, 5.26, 6.92, 7.62, 9.02, 10.08 & 10.62. Each group of data was held as the production set once to evaluate the network performance. The four input variable ranges and the number of patterns in different pH groups are listed in Table 3.6. The only one output was the initial reaction rate of chlorine dioxide. Testing data sets were randomly extracted, which is one third of the amount of training data.

3.3.2.1 Modeling

Like the model developing process for ethanethiol, we compared the performance of different architecture neural networks and optimized network settings: hidden layers, hidden nodes, initial weights, learning rates and momentum. The ANN that had the smallest prediction error still was the standard three-layer back-propagation net with three nodes in the hidden layer. Initial weights, learning rate, and momentum were still 0.1, respectively. To avoid repetition, the selection process is omitted here.

The ANN modeling statistical results on the six production data sets are shown in Table 3.7. The model had relatively large MSE and MAE and low R squared value at the two production data sets: pH 3.58 & 3.61 and 10.08 & 10.62. The average MSE, MAE, and R squared on the other four production data sets (5.26, 6.92, 7.62, and 9.02) are 4.437, 1.589, and 0.8566, respectively.

The ANN model made the best prediction at pH = 5.26. It had the smallest MSE of 0.557 and the smallest MAE of 0.477 as well as the highest R squared value of 0.9757. The linear regression line (y = 1.032x – 0.1836) in Fig. 3.9 shows the model made a very good prediction at this pH. A linear regression line (y = 1.1536x – 2.5994) was fit the data in Fig. 3.10 for the reaction at pH = 6.92. It shows the model tends to slightly under predict the ClO_2 initial reaction rates that are below 18 mg L^{-1} s^{-1} and to slightly over predict the reaction rates that are faster than 18 mg L^{-1} s^{-1}. There is one pattern (with one replicate) that had the largest prediction error (observed value – predicted value = -10 mg L^{-1} s^{-1}) in Fig. 3.10. The other three corresponding input values at this data point are: 500 mg/L DMDS, 66 mg/L ClO_2, and 23°C. While another data point including its two replicates with the similar input values but different ClO_2 concentration (500 mg/L DMDS, 34 mg/L ClO_2, and 23°C) only had a prediction error that is less than 3 mg L^{-1} s^{-1}. The regression line (y = 1.068x + 1.1721) in Fig 3.11 shows that the model over predicted reaction rates at pH = 7.62. In Fig. 3.12, the linear regression line (y = 0.7025x + 3.2628) ANN model over predicted reaction rates below 12 mg L^{-1} s^{-1}, while it under predicted the reaction rates above 12 mg L^{-1} s^{-1}.

As an example, the 149 patterns were randomly partitioned with approximately 35% being placed in model evaluation (53 patterns). The remaining 96 patterns were then used as model development. It was also guaranteed that no patterns with same input values existed in both the training set and the production set. Based on the results of prior model development, the training was stopped when the learning reached 7034 epochs, which is the average learning epochs on the models of pH 5.26, 6.92, 7.62, and 9.02. The MSE, MAE, and R squared value on the production data set are 17.651, 2.827, and 0.9108 respectively. The linear regression line (y = 0.8932x + 1.4299) in Fig. 3.13 shows the model predicted ClO_2 initial reaction rates are very

close to the observed values when the reaction rates are lower than 20 mg L^{-1} s^{-1}, and it tends to slightly under predict the reaction rates when they are faster than 20 mg L^{-1} s^{-1}. Compared to the previous average result on the four production sets (pH 5.26, 6.92, 7.62, and 9.02), the general model has a better performance with a higher R squared value, a lower MAE and MSE.

Fig. 3.14 indicates that the effect of pH on the reaction rates of chlorine dioxide in the reaction with DMDS was not as significant as that in Fig. 3.8. This is consistent with the experimental results since the dissociation of ethanethiol in aqueous solution is determined by pH. All the reaction rates in Fig 3.14 were generated by the model using the same approach as in Fig. 3.8.

3.4 CONCLUSION

Artificial neural network is a good approach to model complex reaction kinetics without the prior knowledge of reaction mechanisms. When only a small data set is available, k-fold cross validation can efficiently use more data in developing models and is more accurate to evaluate model performances. A final model was developed by using all the available patterns as training data set without testing. Stop training when the learning epoch is equal to the average value of the all learning epochs in the k-fold evaluation. To avoid the overfitting problem, a standard three-layer feed-forward network is powerful enough to capture the relationships among inputs and the output. The network model has high accuracy when the prediction is done within the input ranges. The two final models can be used to predict the initial reaction rates of ClO_2 with ethanethiol or DMDS for the future wet scrubber design and optimization.

The prediction accuracy can be improved if more data patterns are available to develop the ANN models. Chemical reaction experiments with more combinations of different initial

chlorine dioxide and VOC concentrations (not necessarily to satisfy the pseudo-first reaction condition) as well as more pH levels can be designed in the future work. Faster response spectrophotometer with an automatic stopped-flow system can be used to reduce noises in the data acquired from very fast reactions.

REFERENCES

Blanco, M., Coello, J., Iturriaga, H., Maspoch, S., and Redon, M., 1995. Artificial Neural Networks for multicomponent kinetic determinations. *Anal. Chem.*, 67, 4477-4483.

Bryjak, J., Murlikiewicz, K., Zbicinski, I., and Stawczyk, J., 2000. Application of artificial neural networks to modeling of starch hydrolysis by glucoamylase. *Bioprocess Engineering*, 23, 351-357.

Bulsari, A., 1995. *Neural networks for chemical engineers*. Amsterdam: Elsevier Science.

Galvan, I. M., Zaldfvar, J. M., Hernandez, H., and Molga, E., 1996. The use of neural networks for fittng complex kinetic data. *Computers and Chemical Engineering*, 20, 1451-1465.

Gasteiger, J., and Zupan, J. (1993). Neural networks in chemistry. *Angew. Chem. Int. Ed. Engl.*, 32, 503-527.

Greenberg, A. E., Clesceri, L. S., and Eaton, A. D., 1992. *Standard methods for the examination of water and wastewater*. Washington: American Public Health Association.

Kastner, J. K., and Das, K. C., 2002. Wet scrubber analysis of volatile organic compound removal in the rendering industry. *Journal of the Air & Waste Management Association*, 52, 459-469.

Kastner, J. K., Hu, C., Das, K. C., and McCelndon, R., 2003. Effect of pH and Temperature on the Kinetics of Odor Oxidation Using Chlorine Dioxide. *Journal of the Air & Waste Management Association*, 53, 1218-1224.

Mitchell, T. M., 1997. *Machine Learning*. Boston: WCB/McGraw-Hill.

Oae, S., 1977. *Organic Chemistry of Sulfur*. New York: Plenum Press.

Psichogios, D. C., and Ungar, L. H., 1992. A hybrid neural network – first principles approach to process modeling. *AIChE Journal*, 38, 1499-1511.

Russell, S., Norvig, P.,1995. *Artificial intelligence: A modern approach*. New Jersey: Prentice Hall.

Safavi, A., Absalan, G., and Maesum S., 2001. Simultaneous determination of V(IV) and Fe(II) as catalyst using "neural networks" through a single catalytic kinetic run. *Analytica Chimica Acta*, 432, 229-233.

Smith, M., 1993. *Neural networks for statistical modeling*. New York: Van Nostrand Reinhold.

Steinfeld, J. I., Francisco, J. S., and Hase, W. L., 1999. *Chemical kinetics and dynamics*. New Jersey: Prentice Hall.

Zupan, J., and Gasteiger, J. (1999). *Neural networks in chemistry and drug design*. Weinheim: Wiley-Vch.

Table 3.1 Input value ranges and the number of patterns in the modeling of ethanethiol and

chlorine dioxide reaction

Inputs		Value range				
Ethanethiol concentration, mg/l		100, 175, 250, 375, 500				
Chlorine dioxide concentration, mg/l		10 - 56				
Temperature, °C		23, 26, 30, 32, 35, 37, 40				
pH	Groups	3.58, 3.61	3.73	3.92	4.01	4.21, 4.55
	Number of patterns	29	12	11	12	25

Table 3.2 Effect of hidden node numbers on the performance of standard nets with one hidden

layer in the modeling of the reaction of chlorine dioxide and ethanethiol.

Hidden node number	MSE	MAE	R squared
2	69.036	5.749	0.5477
3	24.072	3.824	0.6813
4	37.158	4.695	0.5844
5	31.015	4.170	0.5689
7	32.377	4.070	0.5491

Note 1: Initial weights, learning rate, and momentum were all 0.1. Results were the average values on the five production data sets.

Table 3.3 Selection of standard net initial weights in the modeling of chlorine dioxide and

ethanethiol reaction[1]

Initial weights	0.01	0.05	0.1	0.3	0.5
MSE	29.651	26.778	24.072	31.932	34.386
MAE	4.532	4.096	3.824	4.688	4.717
R squared	0.6626	0.6722	0.6813	0.6550	0.6468

Note 1: The ANN had three hidden nodes. Learning rate and momentum were both 0.1. Results were the average values on the five production data sets.

Table 3.4 Effect of learning rates and momentum on the performance of standard nets for the

modeling of chlorine dioxide and ethanethiol reaction[1]

Learning rate	Momentum	MSE	MAE	R squared
0.1	0.01	28.842	4.417	0.6652
0.1	0.05	29.033	4.451	0.6647
0.1	0.1	24.072	3.824	0.6813
0.1	0.3	29.577	4.254	0.6629
0.1	0.5	30.372	4.510	0.6602
0.01	0.1	28.084	4.400	0.6679
0.05	0.1	26.034	4.099	0.6747
0.3	0.1	25.549	3.981	0.6764
0.5	0.1	30.261	4.355	0.6606

Note 1: The ANN had three hidden nodes. Initial weights were 0.1. Results were the average values on the five production data sets.

Table 3.5 Statistics of the prediction of chlorine dioxide initial reaction rates with ethanethiol

using a standard back-propagation ANN

pH	3.58, 3.61	3.73	3.92	4.01	4.21, 4.55
MSE	20.804	6.433	21.156	25.833	67.415
MAE	3.315	2.084	4.195	4.135	6.733
R squared	0.2322	0.9484	0.9060	0.9294	0.7319

Table 3.6 Input value ranges and number of patterns in the modeling of DMDS and chlorine

dioxide reaction

Inputs		Value range					
DMDS concentration, mg/l		100, 175, 188, 250, 375, 500					
ClO$_2$ concentration, mg/l		4 - 79					
Temperature, °C		23, 26, 30, 32, 35, 37, 40					
pH	Groups	3.58, 3.61	5.26	6.92	7.62	9.02	10.08, 10.62
	Number of patterns	29	12	28	18	26	36

Table 3.7 Statistics of the prediction of chlorine dioxide initial reaction rates with DMDS using

a standard back-propagation ANN

pH	3.58, 3.61	5.26	6.92	7.62	9.02	10.08, 10.62
MSE	129.628	0.557	8.672	3.058	5.459	159.243
MAE	6.872	0.477	2.405	1.562	1.911	10.780
R squared	0.6764	0.9757	0.8276	0.8063	0.8168	0.5724
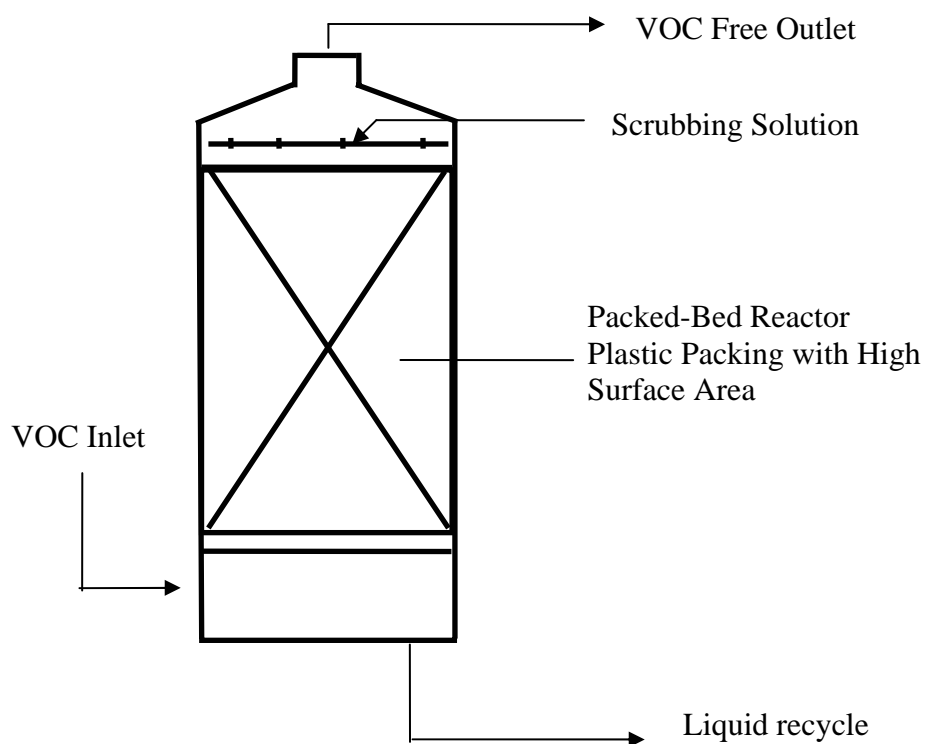
Fig. 3.1 Wet scrubber system
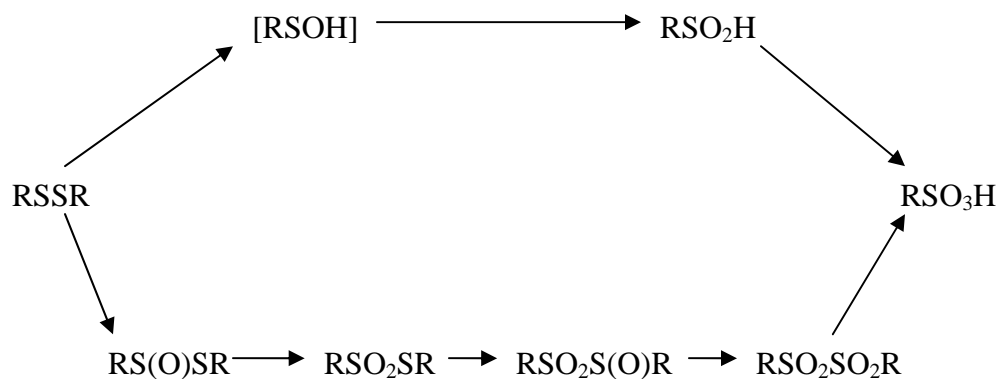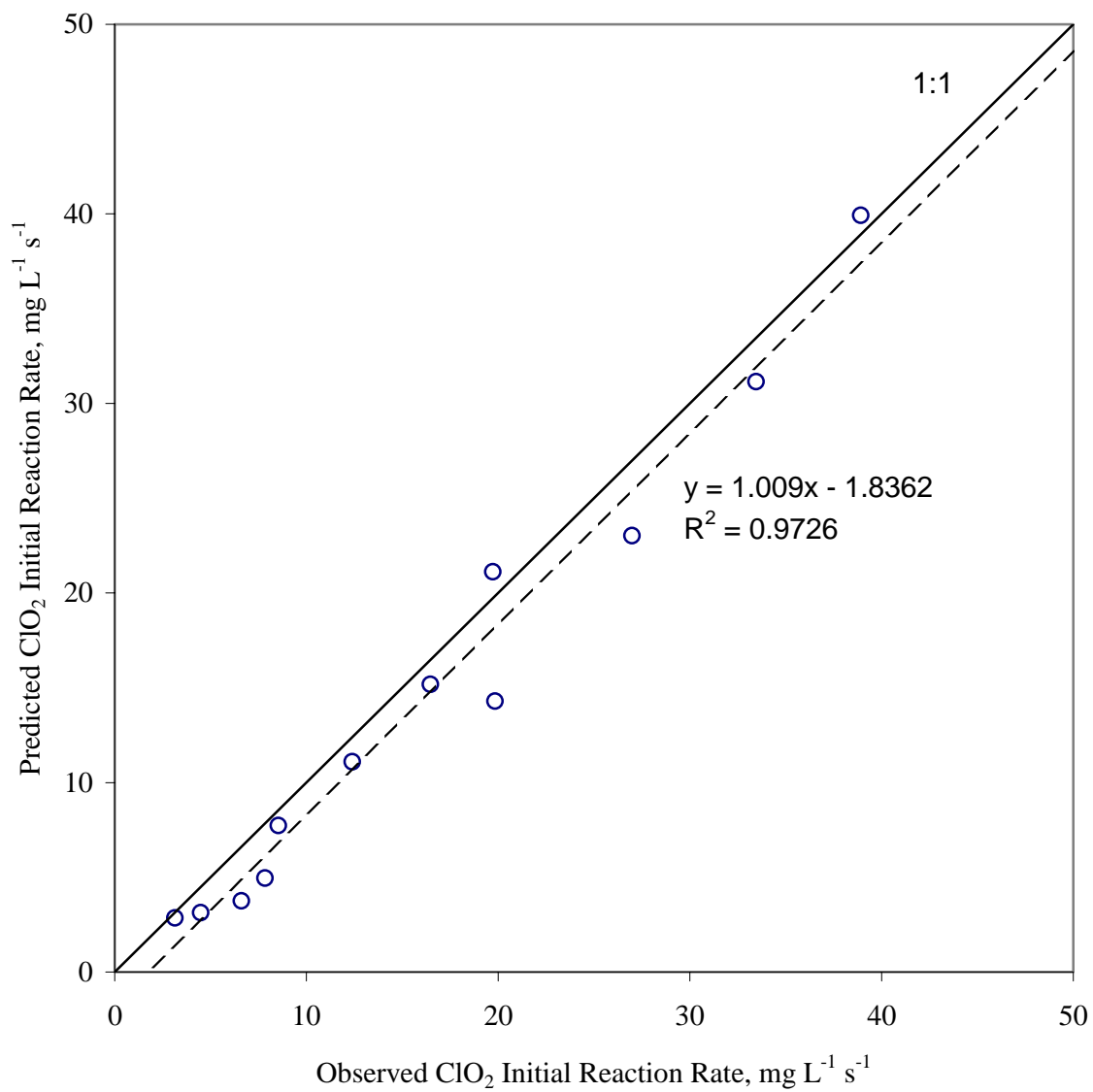

Fig. 3.2 Oxidation of disulfide (Oae, 1977)

Input layer   Hidden Layer   Output layer

VOC

Bias

ClO$_2$

pH

Temp

Reaction rate

Linear function   Logistic function   Logistic function

Fig. 3.3 Topology of a three-layer feed-forward neural network, activation functions for nodes in each layer.

Fig. 3.4 Prediction of ClO_2 initial reaction rates with ethanethiol at pH=3.73
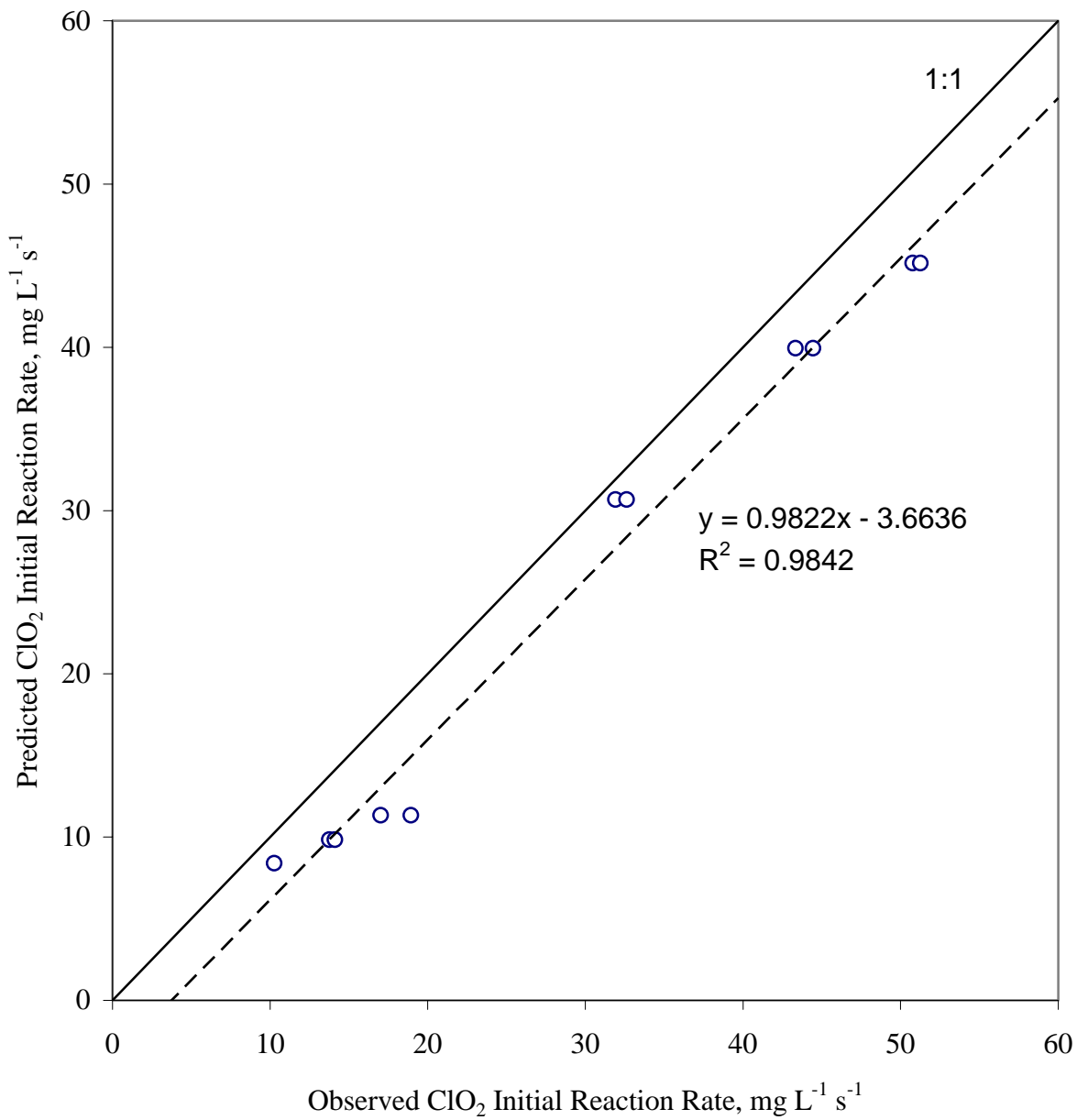
Fig. 3.5 Prediction of ClO_2 initial reaction rates with ethanethiol at pH = 3.92
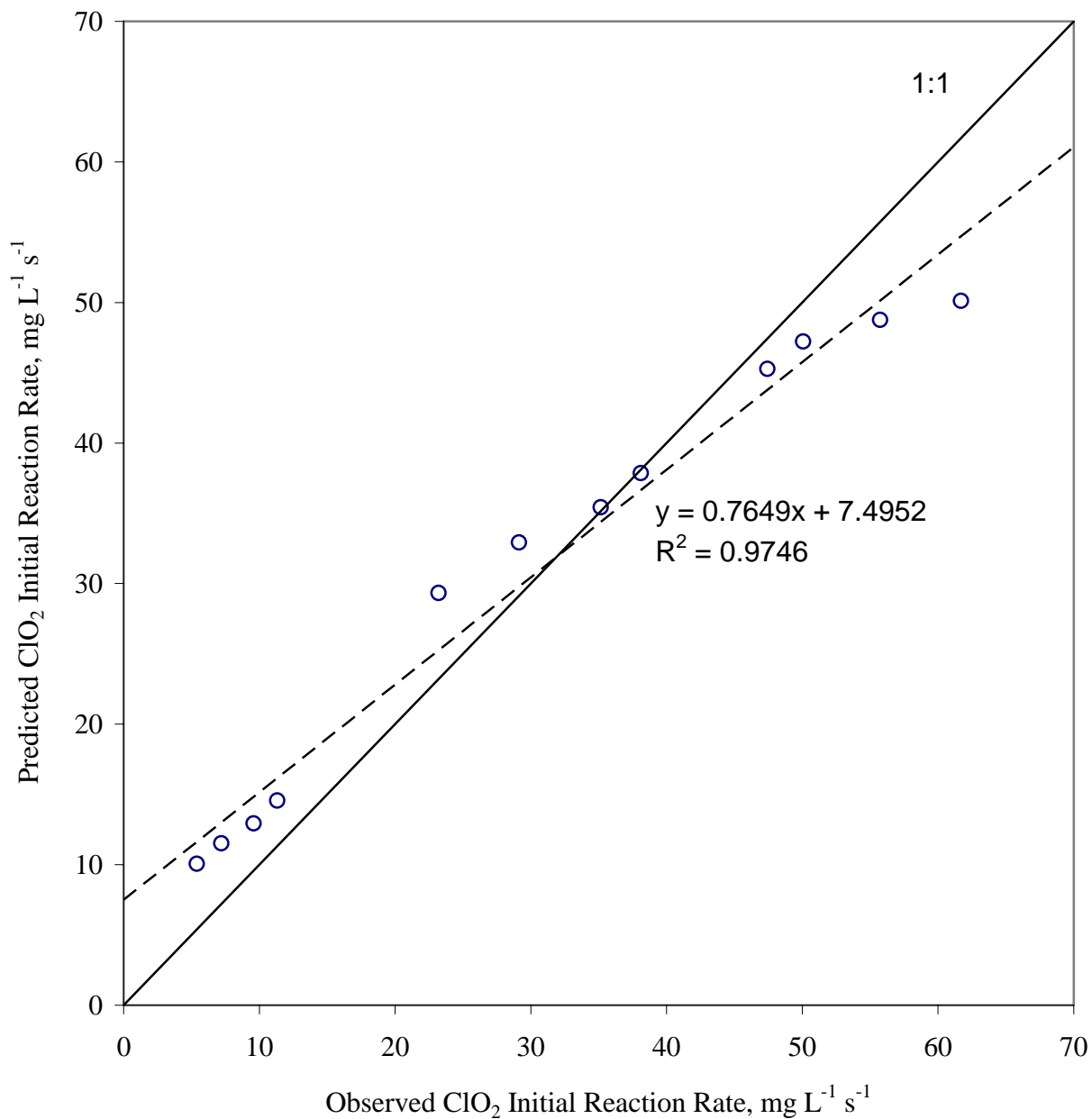
Fig. 3.6 Prediction of ClO_2 initial reaction rates with ethanethiol at pH=4.01
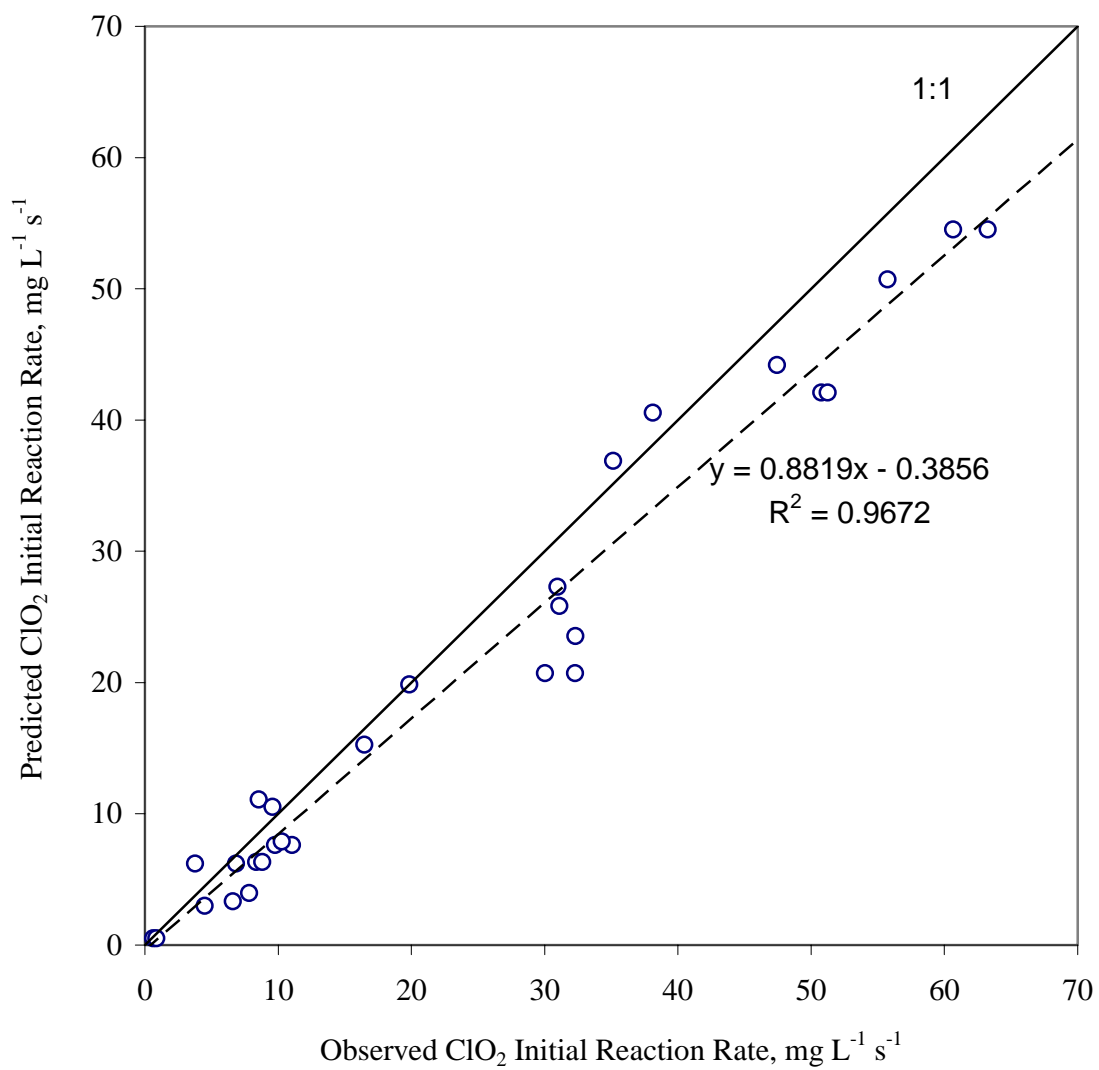
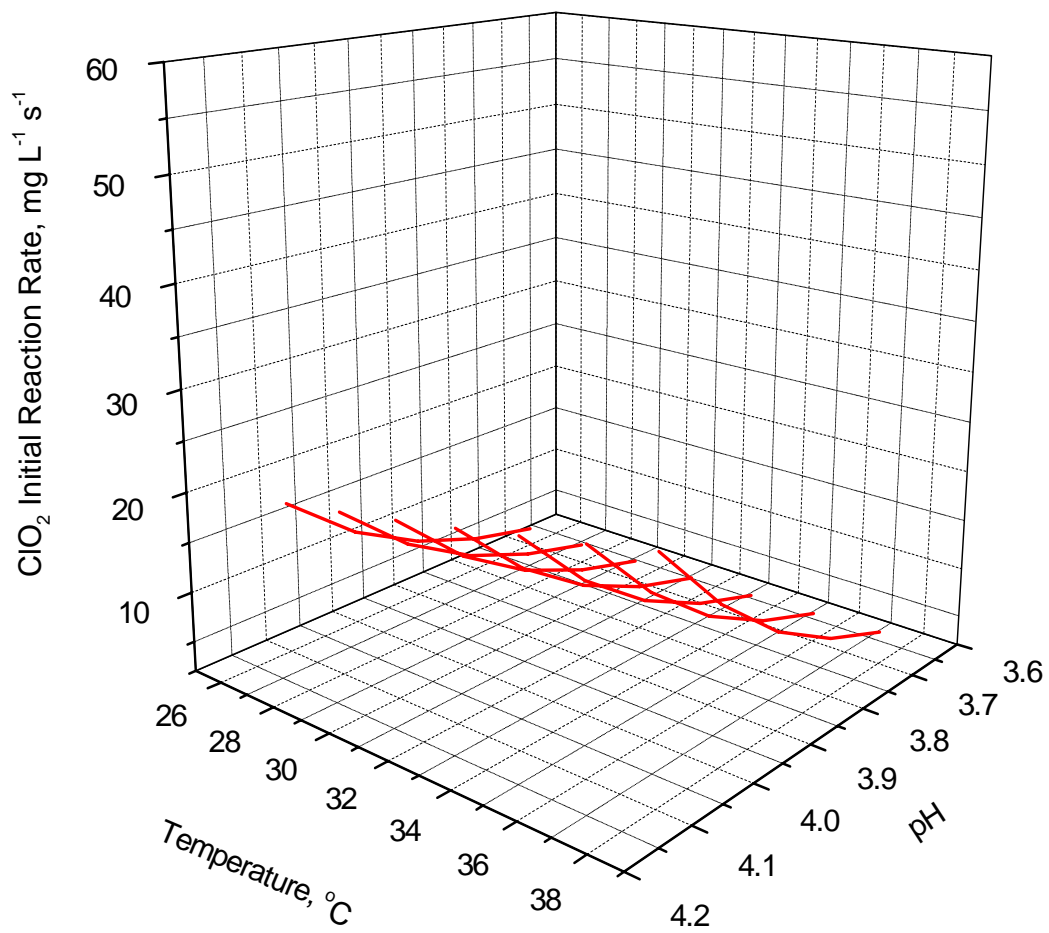Fig. 3.7 Prediction of ClO_2 initial reaction rates with ethanethiol, general model
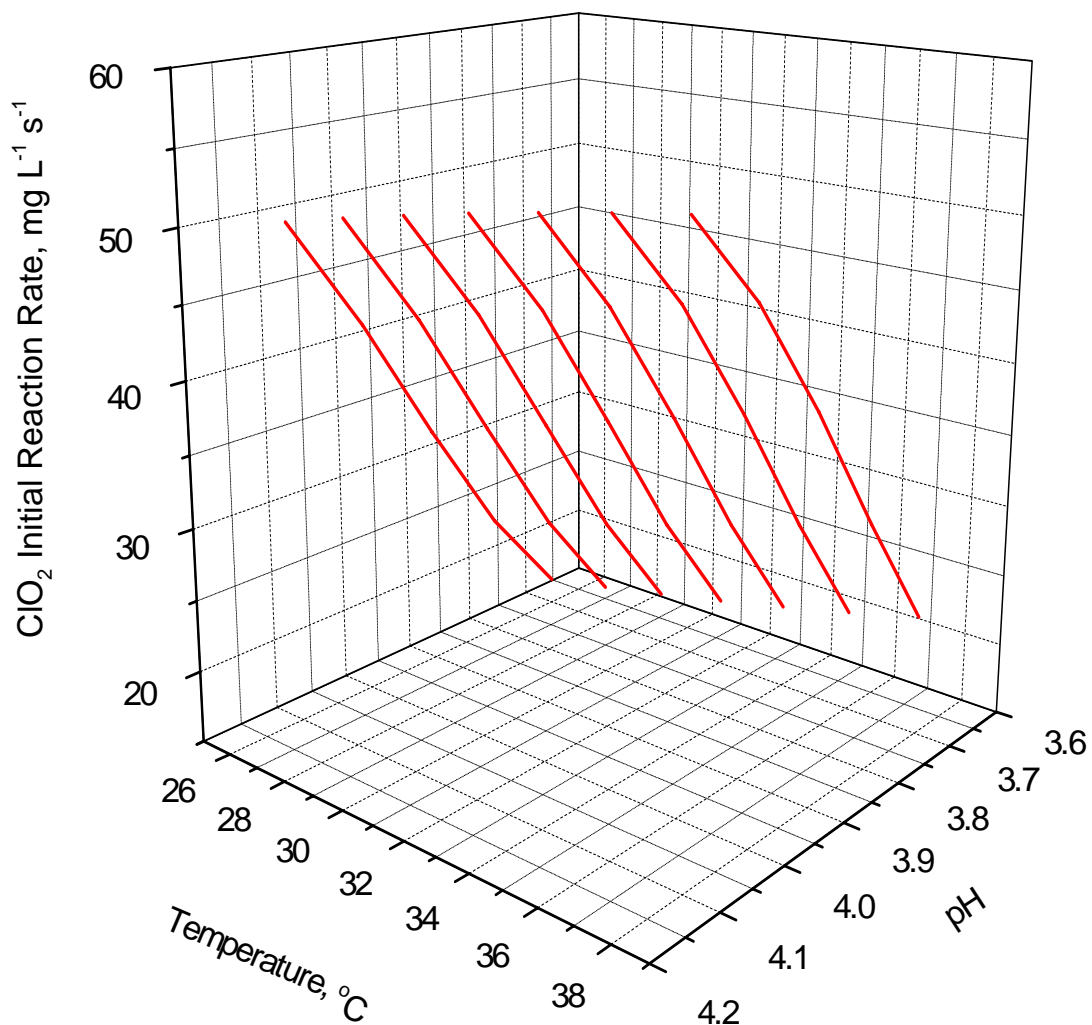
Fig. 3.8 (a)

Fig. 3.8 (b)

Fig. 3.8 Effects of temperature and pH on the initial reaction rate of chlorine dioxide with ethanethiol. Initial concentrations of ethanethiol and ClO_2 in (a) were 175 mg/L and 20 mg/L. In (b), they were 375 mg/L and 40 mg/L.
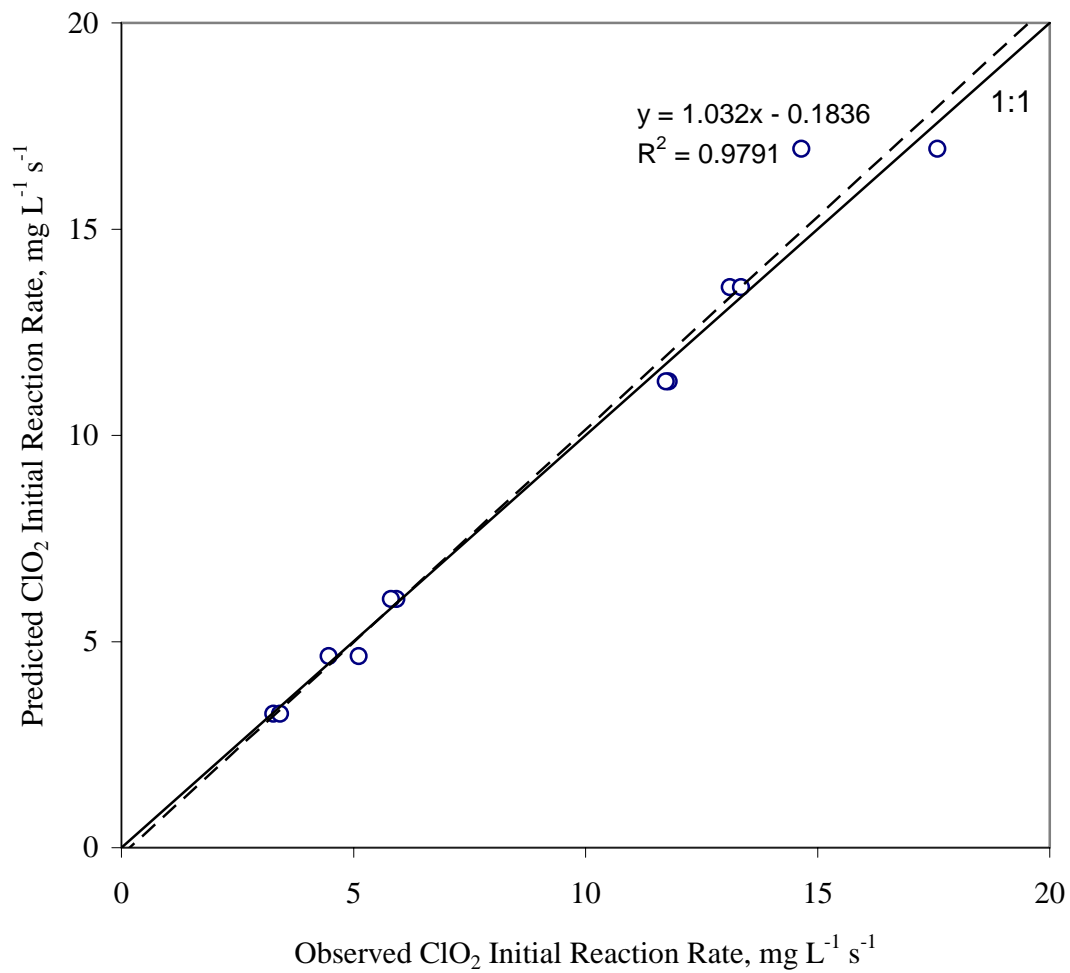
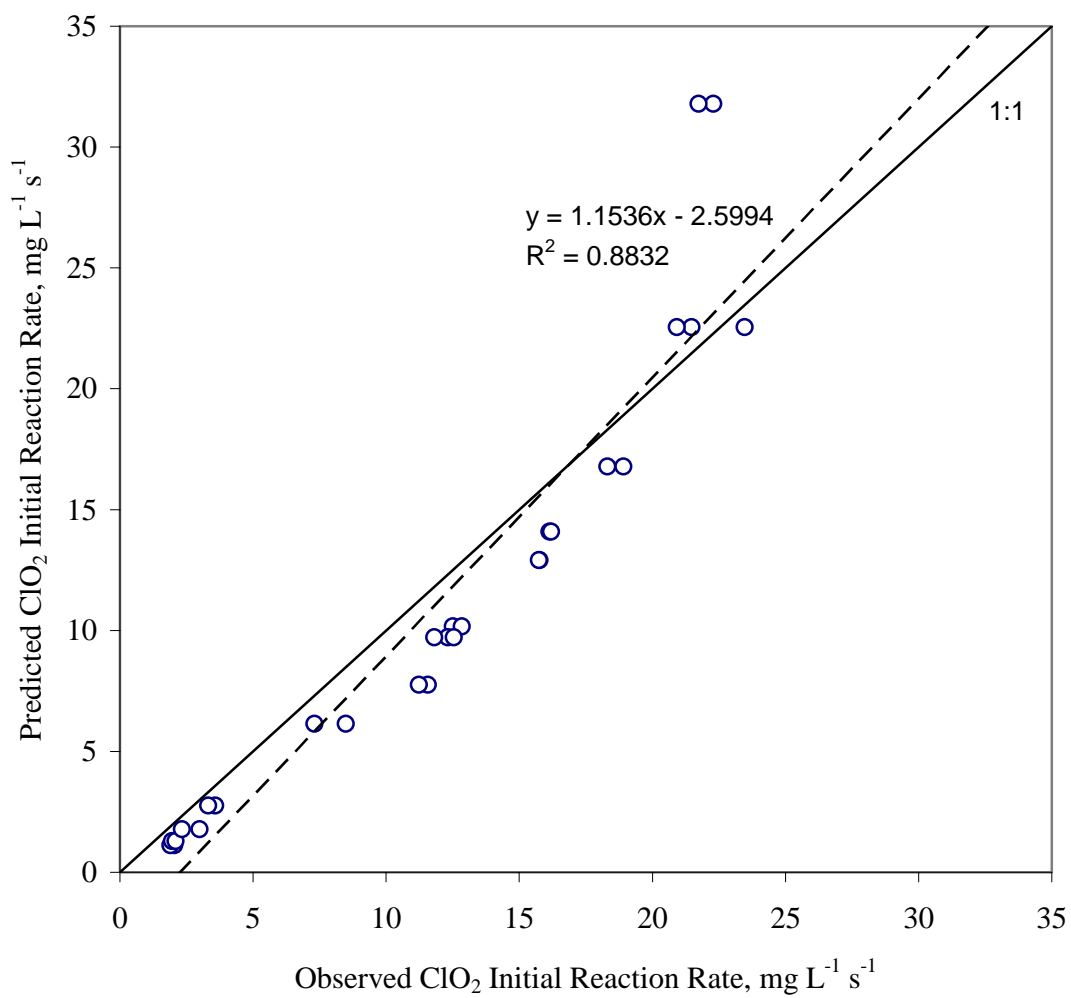Fig. 3.9 Prediction of ClO_2 initial reaction rates with DMDS at pH = 5.26

Fig. 3.10 Prediction of ClO_2 initial reaction rates with DMDS at pH = 6.92

The figure contains the following labels and annotations:

- y-axis: Predicted ClO_2 Initial Reaction Rate, mg L^{-1} s^{-1}
- x-axis: Observed ClO_2 Initial Reaction Rate, mg L^{-1} s^{-1}
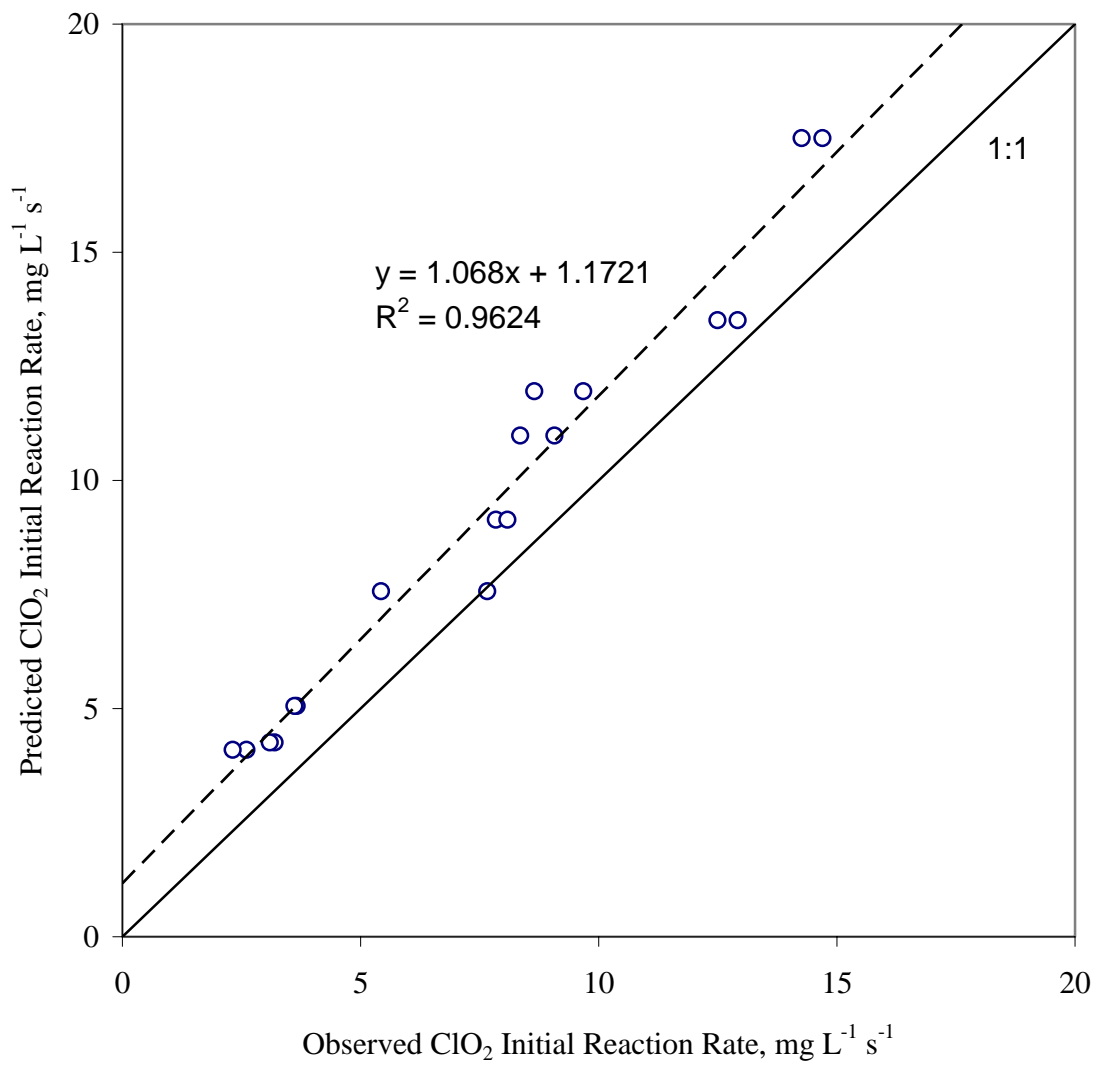- $y = 1.1536x - 2.5994$
- $R^2 = 0.8832$
- 1:1

Fig. 3.11 Prediction of ClO_2 initial reaction rates with DMDS at pH = 7.62
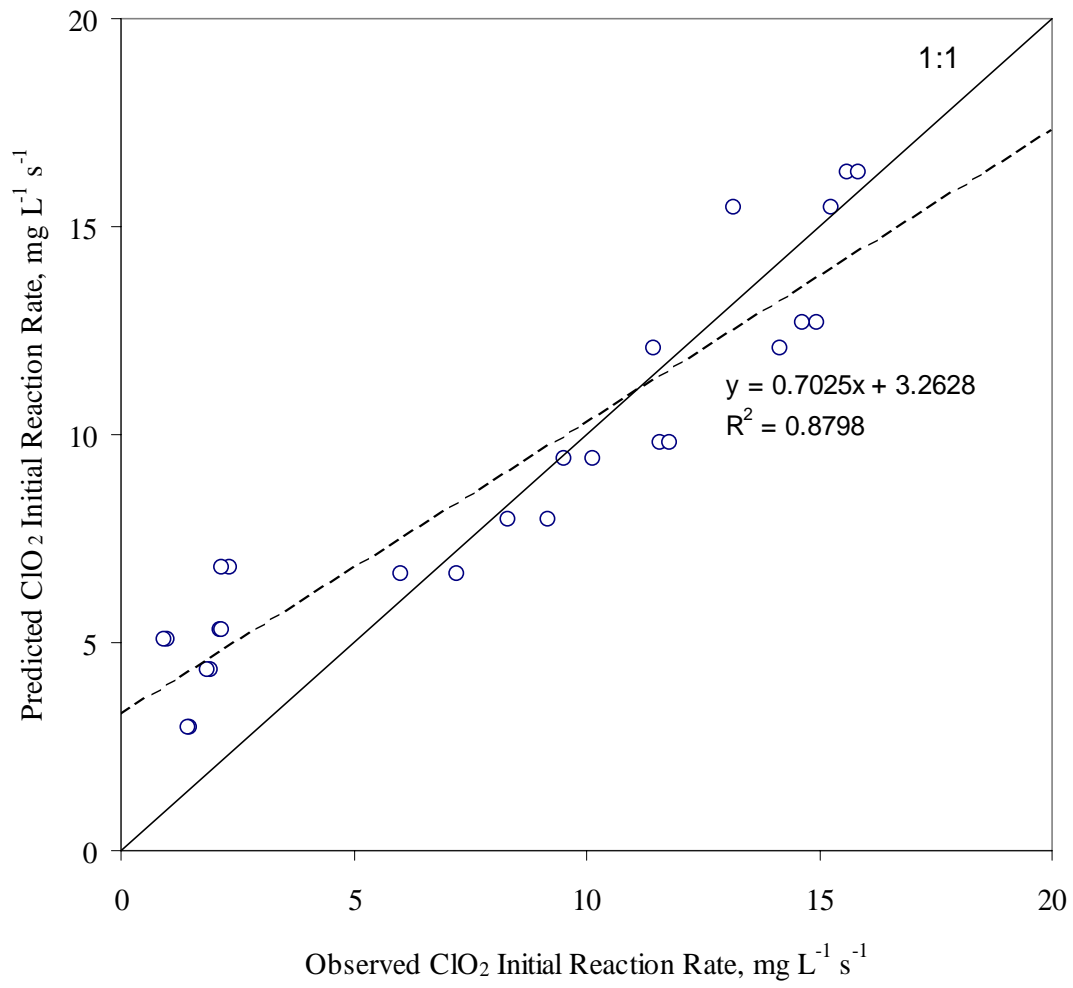
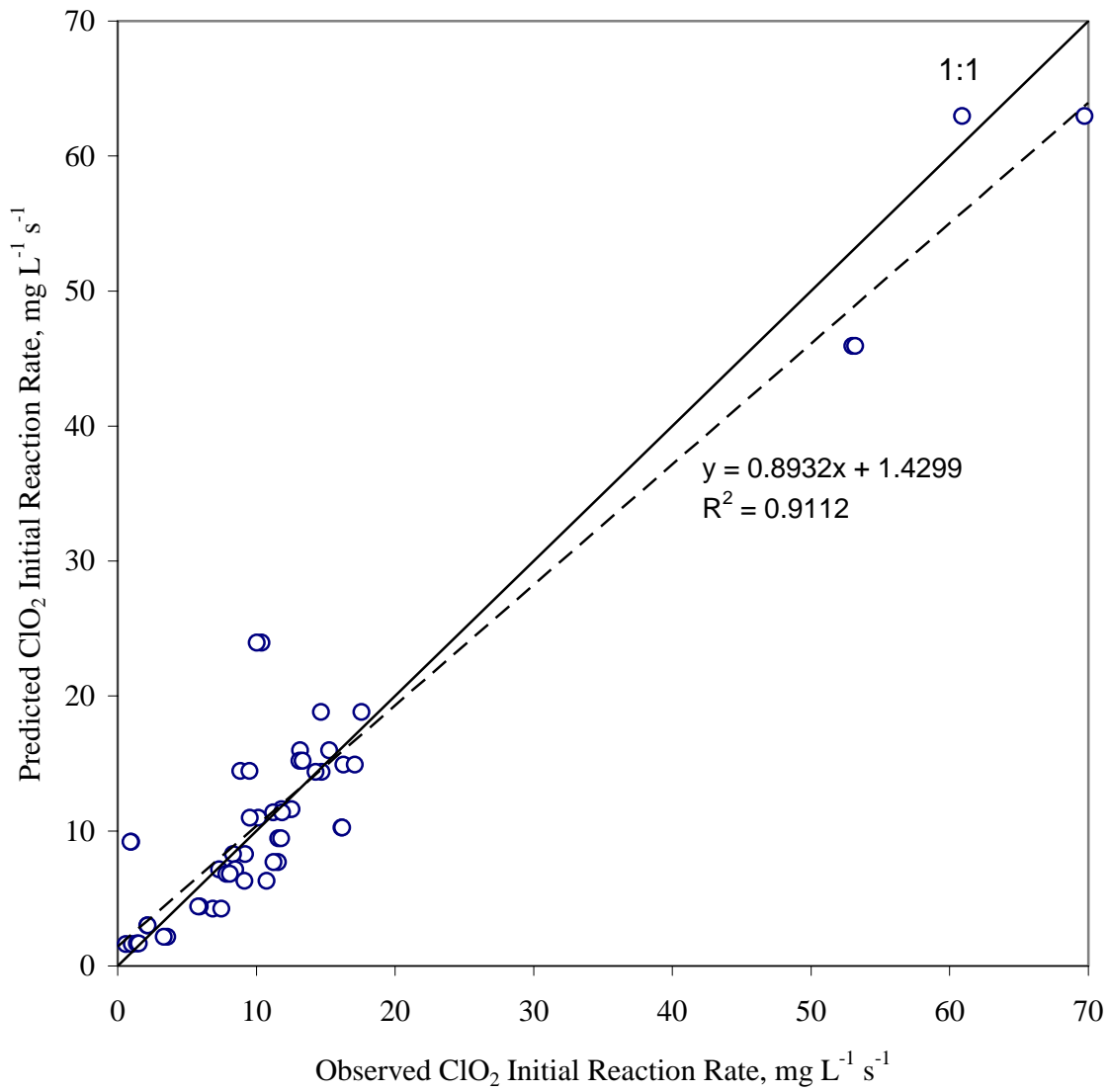Fig. 3.12 Prediction of ClO_2 initial reaction rates with DMDS at pH = 9.02

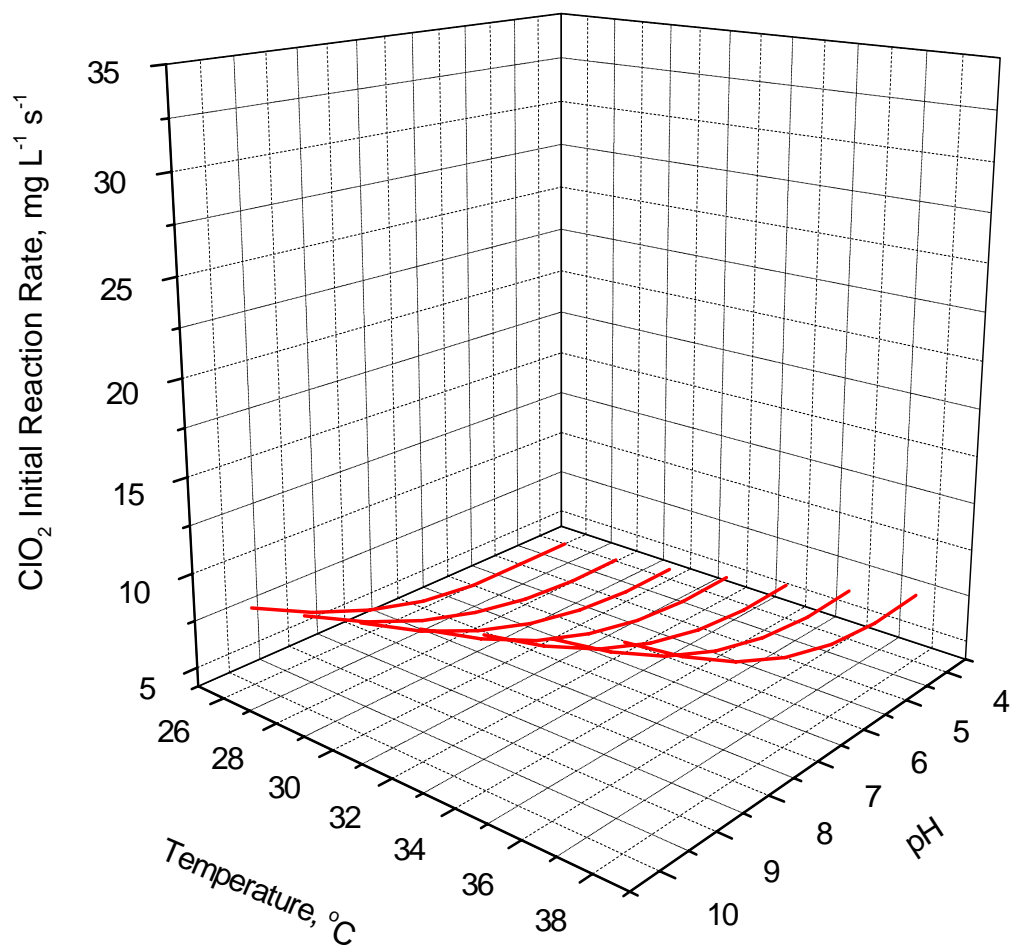Fig. 3.13 Prediction of ClO_2 initial reaction rates with DMDS, general model
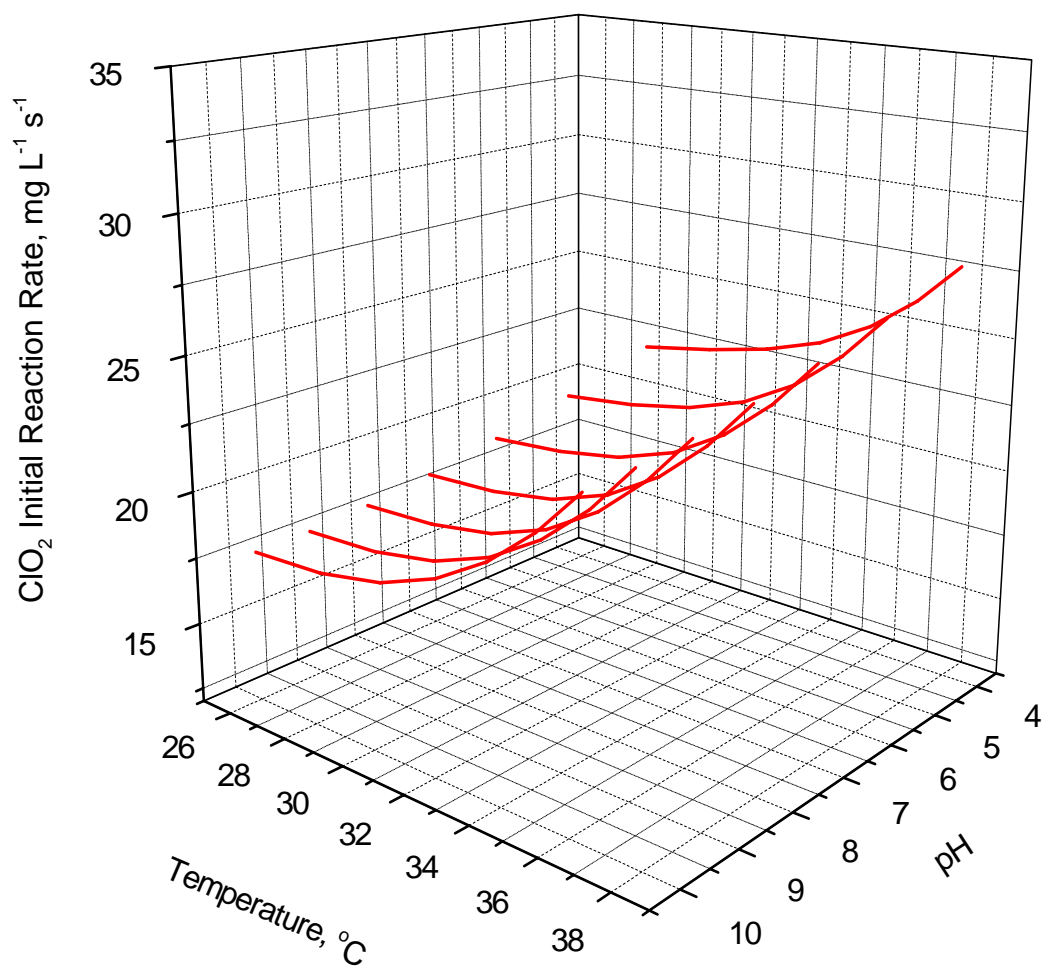
Fig. 3.14 (a)

Fig. 3.14 (b)

Fig. 3.14 Effects of temperature and pH on the initial reaction rate of chlorine dioxide with DMDS. Initial concentrations of DMDS and ClO_2 in (a) were 175 mg/L and 20 mg/L. In (b), they were 375 mg/L and 40 mg/L.

CHAPTER 4

MODELING REACTION KINETICS OF CHLORINE DIOXIDE AND MIXTURES OF

VOLATILE ORGANIC COMPOUNDS

4.1 Introduction

As mentioned in Chapter 3, major VOCs identified in rendering emissions include

DMDS, methanethiol, octane, hexanal, 2-methylbutanal, 3-methylbutanal, and 2-methylpropanal

(Kastner and Das, 2002). In Chapter 2, we found that these aldehydes do not react with chorine

dioxide at the normal reaction conditions. However, if the reaction kinetics of chlorine dioxide

and VOC mixtures, such as ethanethiol and DMDS, can be modeled then these results can be

used to design and optimize wet scrubbers. What we want to know most is the reaction rates of

each VOC component respectively during the reaction, but it is difficult to directly measure the

concentration change of the VOC component. Although ethanethiol absorbs lights in the organic

solvent, heptane, at 229 nm with a very low molar absorption coefficient of 165 (Perkampus,

1992), we did not observe any absorption in a water solution in the wavelength range from 200

nm to 400 nm. DMDS absorbs at 252 nm in water solutions, but the molar absorption coefficient

also is very low. It has absorptions at 254 nm in 96% ethanol with a molar absorption coefficient

of 275 (Perkampus, 1992). Moreover, one of the intermediate oxidation products of ethanethiol

is also a disulfide, which will cause absorption overlap with DMDS in the mixtures. Given the

potential interference of the oxidized by-products on the determination of ethanethiol and

DMDS, and our inability to measure the by-products, we measured the absorption of chlorine dioxide to calculate the reaction rate.

The reaction of chlorine dioxide and VOC mixtures are more complicated than the reaction of single VOC component. It involves parallel reactions, consecutive reactions, and competitive reaction steps (Zuman and Patel, 1984; Steinfeld et al., 1999). Given the complexity and non-linearity of such a system, we proposed to use ANNs to model the reaction. Actually, some researchers have used ANNs in the modeling of multiple component mixture reaction kinetics. Blanco et al. (1995) applied ANNs to model multiple component mixture reaction kinetics. They used the scores of a principle component model as input data to the ANN model and compared the ANN approach with two traditional statistical methods: projection to latent structures (PLS) and principle component regression (PCR). Both linear and non-linear systems were tested by these three methods. The results provided by the three methods on linear system were comparable, but in non-linear systems, the ANN method clearly outperformed the other two. Galvan et al. (1996) discussed the use of ANNs for fitting complex kinetic data. In their case studies, they compared the ANN approach with traditional kinetic identification methods. Their results showed that ANNs could be used to deal with the fitting of complex kinetic data to obtain an approximate reaction rate function in a limited amount of time, which can be used for design improvement or optimization.

All the kinetic data of the reaction of chlorine dioxide with ethanethiol and DMDS mixtures were acquired in a Hi-Tech KinetAsyst™ Stopped Flow System (Hi-Tech Scientific, model SF-61SX2), a computer controlled instrument for the study of rapid reaction kinetics. Two regents can be rapidly mixed in the sample handling unit and reactions with time courses from a few milliseconds to several seconds can be monitored. A Deuterium (UV) lamp was used and the

wavelength range for UV single shot mode was from 190 nm to 380 nm. For most reactions, the typical instrument parameter settings were: 100 data points, 249 oversample, 0.1 ms filter time, and 10-20 seconds run time. For several very fast reactions at high pH, the filter time was changed to 0.01 ms (minimum value) and the run time was shortened to 1~5 seconds. The goal of this chapter was to use ANNs to model reaction kinetics of chlorine dioxide and the mixtures of ethanethiol and DMDS on bench scales.

4.2 Modeling

The four input ranges and number of patterns in different pH groups are listed in Table 4.1. Reaction temperature was fixed at 30°C. The ANN output was the initial reaction rate of chlorine dioxide. A total of 159 patterns (including replicates) are available to develop and evaluate ANN models. Similar to Chapter 3, all the data were partitioned according to pHs into training, testing, and production sets. When we tried to use 4-fold cross-validation method to develop and evaluate ANN models, we found that the ANN models with many architectures predicted very poorly at the pH boundary values (R squared is zero) by extrapolations. ANN models predicted reaction rates for the mixtures with higher R squared value when interpolating. So, we only used two pH production sets, 4.72 and 5.80, to evaluate ANN models.

Through network architecture selection and parameter optimization, we found that Ward nets (Fig. 4.1) had the smallest prediction error on the two production data sets (pH 4.72 and 5.80). Table 4.2 shows the effect of different hidden node numbers on the performance of the Ward net. The performance of six hidden nodes had no big difference with four hidden nodes, so four hidden nodes were used for all hidden layers in the Ward net. The optimized learning rate, momentum, and initial weights were 0.1, 0.1, and 0.1. Therefore, a Ward net with six hidden

nodes in each hidden layer and above parameter settings were used for all the following model development. Table 4.3 shows the final model prediction statistic results on the four production data sets. The model performance degraded significantly when the predictions were made by extrapolation at the boundary pH values.

The Ward net predicted better at pH = 5.80 than pH = 4.72, as shown in Fig. 4.2 and Fig. 4.3. In Fig. 4.2, the predicted reaction rates scatter around the 1:1 line. While in Fig. 4.3, predicted data points are more close to the 1:1 line. The R squared value for the pH = 5.80 production set is much higher than the latter. MSE and MAE at pH = 5.80 are also higher because the absolute reaction rate is increased at high pH values.

An additional ANN model was developed by randomly partitioning the 159 patterns into a training set (70 patterns), a testing set (39 patterns), and a production set (50 patterns). To avoid the situation that one pattern is in the production set while its replicates is in the training or testing set, we manually examined each pattern in the production set. If we find replicates are separated, then put them together back in the training data set. We also found that the production data set included all the four pH levels. Training was stopped when the ANN had the smallest error on the testing set. As shown in Table 4.3, the model had the best performance with the highest R squared value. Fig. 4.4 shows the observed reaction rate versus the predicted reaction rate.

The reason that we needed more complicated networks to model the reaction of chlorine dioxide and the mixtures of ethanethiol and DMDS but did not achieve better performance compared with the models of single VOC compound may lie in two facts. First, the oxidation of VOC mixtures is more complicated than the oxidation of single VOC compounds, because more reaction steps and more intermediate products are involved. Secondly, the number of available

70

data patterns to develop and evaluate the ANN model was limited (most patterns had two replicates). Furthermore, pH is an important factor (ethanethiol and DMDS have different pH sensitivities), but there are only four different pH values for the model development and evaluation.

4.3 Conclusion

The reaction of chlorine dioxide with mixtures of ethanethiol and DMDS is more complicated than the reaction involves only single VOC component. Ward nets with four hidden nodes in each hidden layer have been used in order to model the reaction kinetics, whereas in Chapter 3, we only need to use a standard 3-layer back-propagation ANN to model the reaction of single VOC compound. As stated in Chapter 2, pH has great influence on the oxidation rate of ethanethiol and DMDS. For mixtures, there are only four different pH levels available for developing and evaluating ANN models. Therefore, the network prediction was not as good as the results for single compound. To improve the model accuracy, more patterns are needed to develop and evaluate the ANN model.

REFERENCES

Blanco, M., Coello, J., Iturriaga, H., Maspoch, S., and Redon, M., 1995. Artificial Neural Networks for multicomponent kinetic determinations. *Anal. Chem*., 67, 4477-4483.

Galvan, I. M., Zaldfvar, J. M., Hernandez, H., and Molga, E., 1996. The use of neural networks for fittng complex kinetic data. *Computers and Chemical Engineering*, 20, 1451-1465.

Kastner, J. K., and Das, K. C., 2002. Wet scrubber analysis of volatile organic compound removal in the rendering industry. *Journal of the Air & Waste Management Association*, 52, 459-469.

Perkampus, H., 1992. *UV-VIS atlas of organic compounds (second edition).* Weinheim: VCH Verlagsgesellschaft mbH.

Steinfeld, J. I., Francisco, J. S., and Hase, W. L., 1999. *Chemical kinetics and dynamics*. New Jersey: Prentice Hall.

Zuman, P., Patel, R. C., 1984. *Techniques in organic reaction kinetics*. New York: John Wiley & Sons, Inc.

Table 4.1 Input ranges in the reaction modeling of chlorine dioxide and mixtures of ethanethiol and DMDS (reaction temperature 30°C)

Inputs		Value range			
Ethanethiol concentration, mg/l		0, 5, 10, 15, 20			
DMDS concentration, mg/l		0, 5, 10, 15, 20			
Chlorine dioxide concentration, mg/l		29 - 91			
pH	Groups	3.71	4.72	5.80	7.03
	Number of patterns	39	45	45	30

Table 4.2 Effect of hidden node number on the performance of Ward nets in the modeling of the reaction of chlorine dioxide and mixtures of ethanethiol and DMDS (pH = 4.72 and 5.80)

Hidden node number	MSE	MAE	R squared
3	62.433	6.657	0.3731
4	45.026	5.392	0.4670
6	38.685	5.159	0.4183

Table 4.3 Modeling statistics of the reaction of chlorine dioxide and VOC mixtures

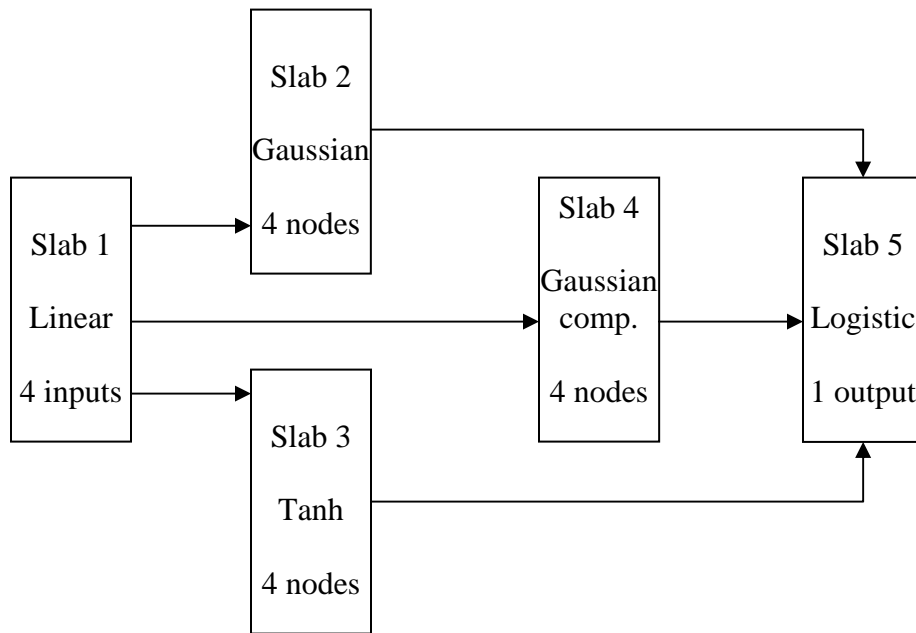| pH	3.71	4.72	5.80	7.03	Random partition
MSE	3.856	19.718	70.333	602.959	13.638
MAE	1.713	3.635	7.149	22.062	2.274
R squared	0	0.1530	0.7809	0	0.8753

Fig. 4.1 Topology of a Ward net, activation functions, and nodes in each layer
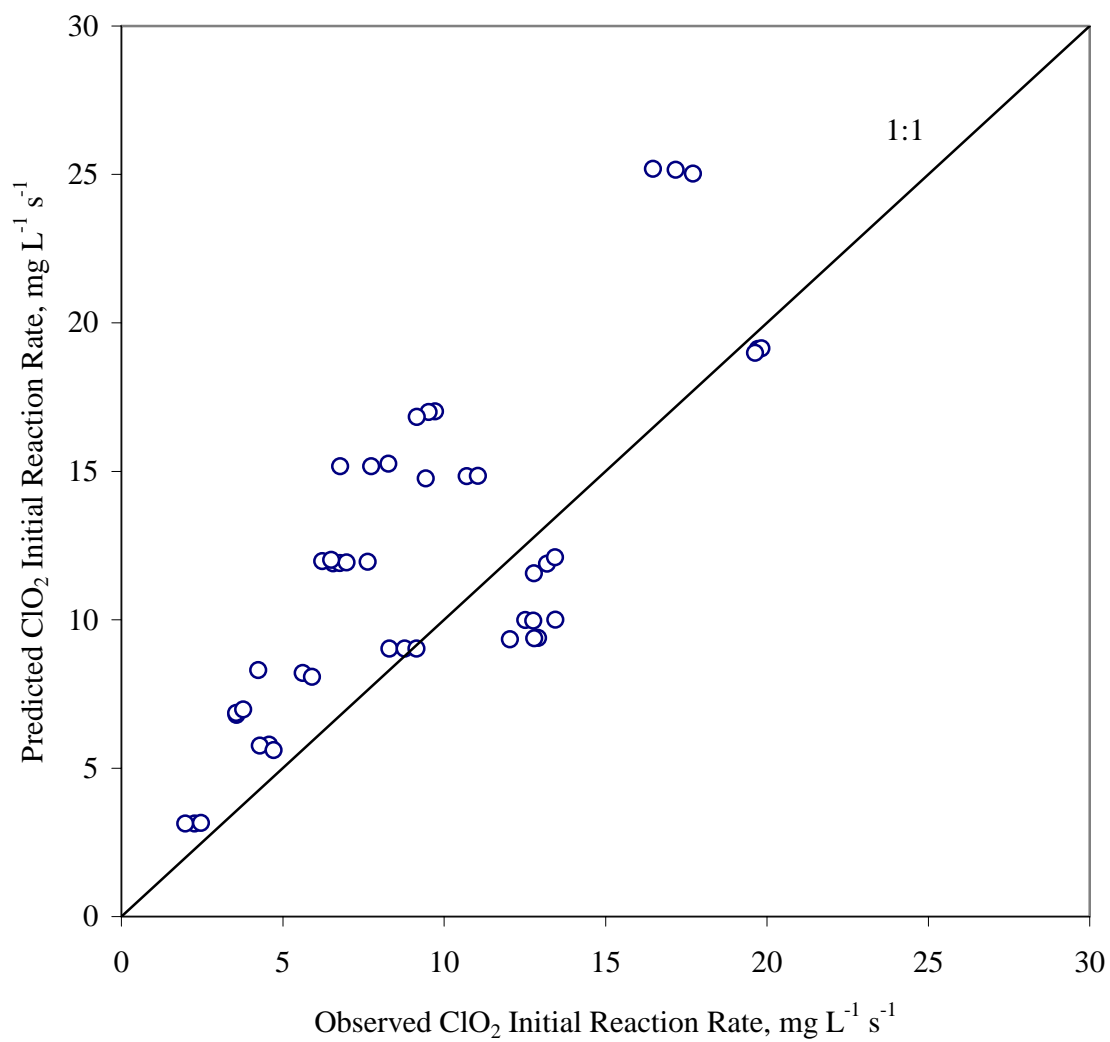
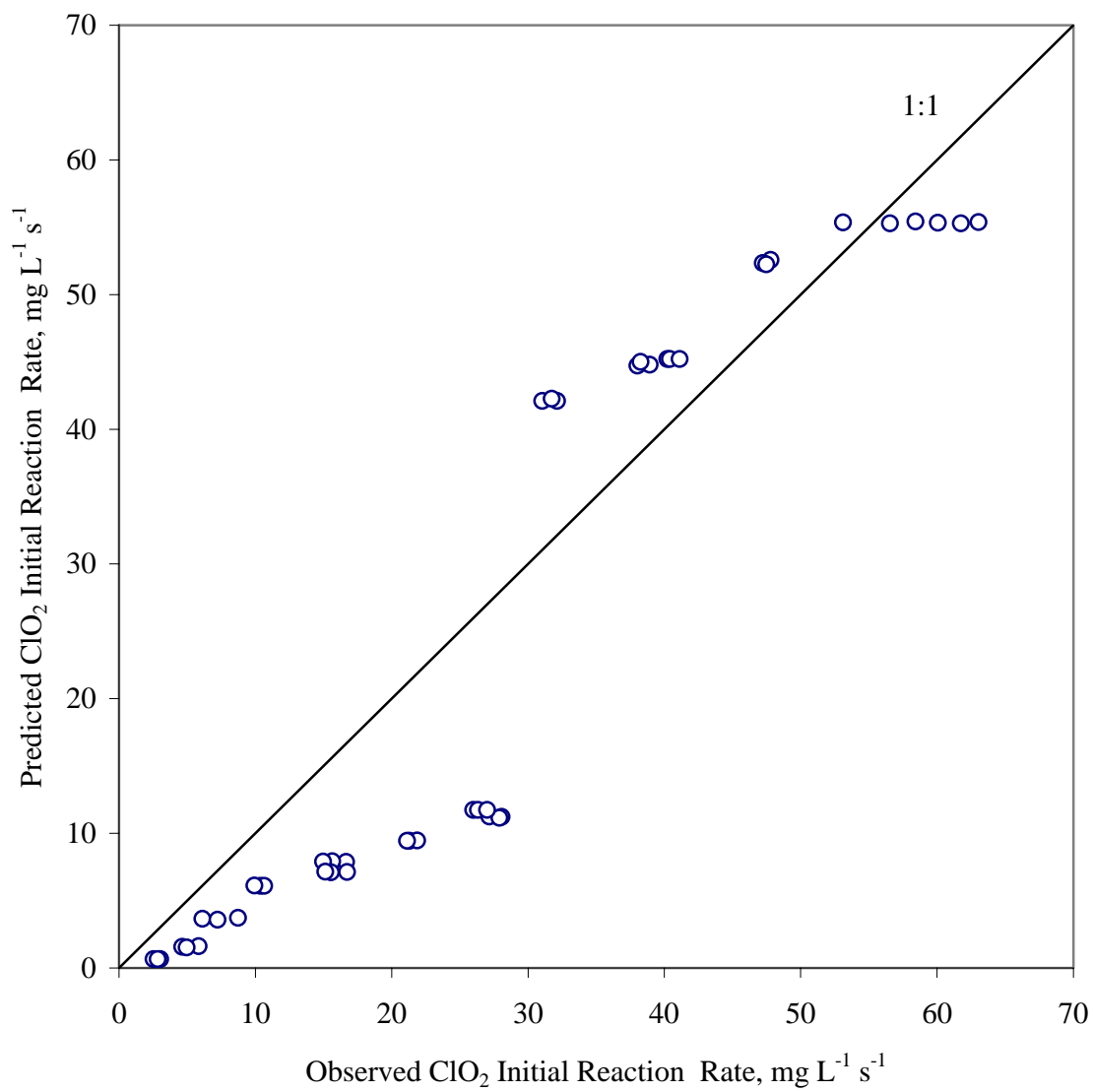Fig. 4.2 Prediction of ClO$_2$ initial reaction rates with ethanethiol and DMDS mixtures at pH=4.72

Fig. 4.3 Prediction of ClO$_2$ initial reaction rates with ethanethiol and DMDS mixtures at pH = 5.80
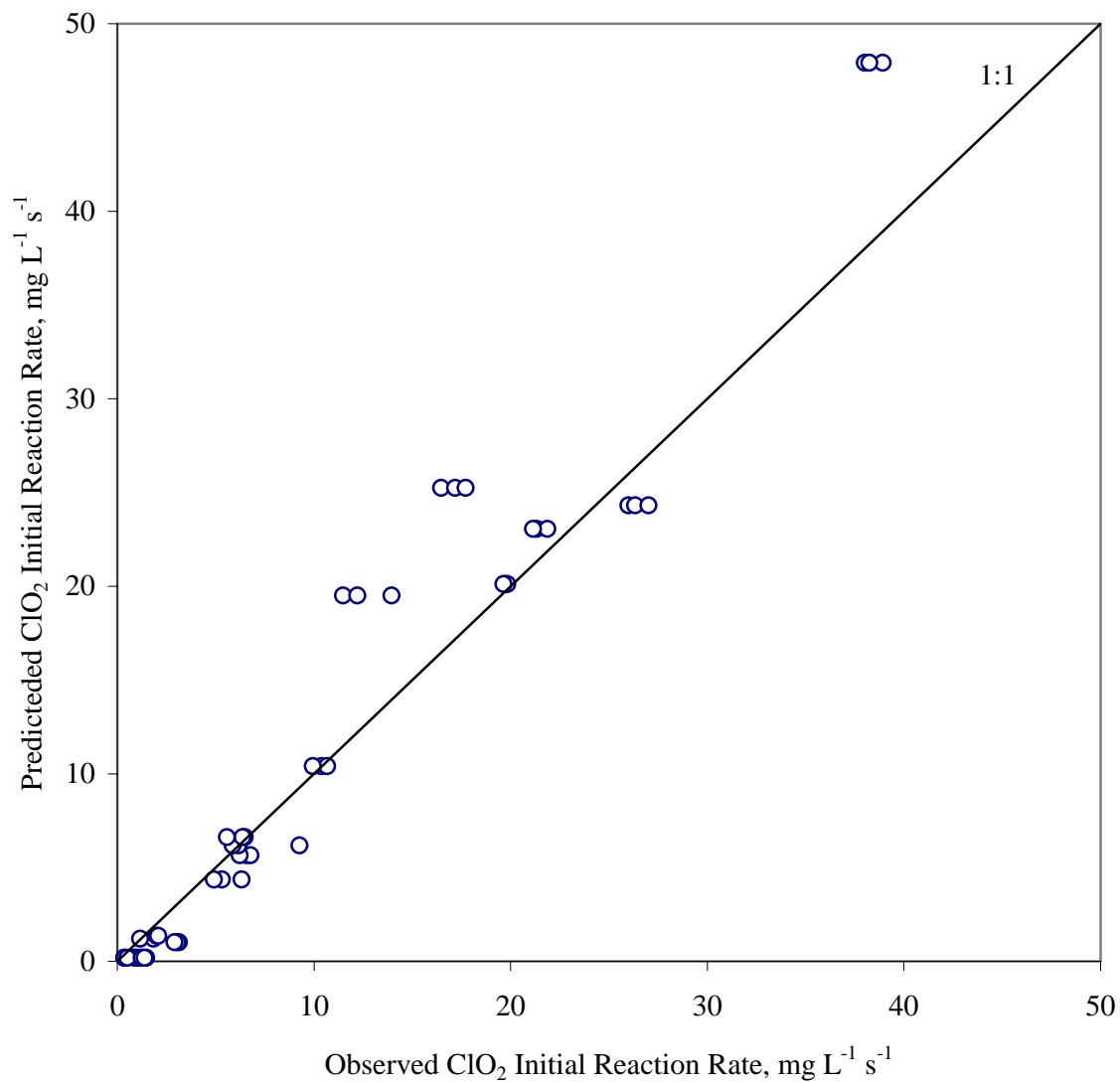
Fig. 4.4 Prediction of ClO_2 initial reaction rates with ethanethiol and DMDS mixtures, randomly partitioning data.

CHAPTER 5

CONCLUSIONS AND FUTURE WORK

The kinetic analysis indicated that chlorine dioxide does not react with hexanal and 2-methylbutanal over a wide range of pH and temperatures, which constitutes a major fraction of VOC emissions. Contrary to the aldehydes, ethanethiol and dimethyl disulfide rapidly reacted with ClO_2. Moreover, an increase in pH from 3.6 to 5.05 exponentially increased the reaction rate of ethanethiol and significantly increased the reaction rate of dimethyl disulfide if increased to pH 9. Thus, a small increase in pH could significantly improve wet scrubber operations for removal of odor causing compounds. The results explain why aldehyde removal efficiencies are much lower than methanethiol and DMDS in wet scrubbers using ClO_2. The overall order of the reaction of chlorine dioxide and ethanethiol is a second-order reaction. For dimethyl disulfide, it is a third-order oxidation reaction. Incorporating oxidation kinetics into a wet scrubber model predicted increasing removal efficiency with increasing pH (i.e., reaction rate) but did not adequately predict results in an industrial scale scrubber.

ANNs are a good approach to model complex reaction kinetics without the prior knowledge of reaction mechanisms. When only a small data set is available, k-fold cross validation can efficiently use more data in developing models and is more accurate to evaluate model performances. For the reaction of chlorine dioxide with single VOC compounds, such as ethanethiol or dimethyl disulfide, a standard three-layer feed-forward network with back-

78

propagation learning was powerful enough to capture the relationships among the reaction conditions and the initial reaction rate of chlorine dioxide. The network model had higher accuracy when the prediction was done by interpolation. Its performance degraded at boundary values.

The reaction of chlorine dioxide with mixtures of ethanethiol and DMDS is more complicated than the reaction involves single VOC component. Ward nets with four hidden nodes in each hidden layer had been used in order to better model the reaction kinetics. Because the data for developing and evaluating the ANN model is limited, especially the available pH levels, the network prediction was not as good as the results for the single VOC compound. Further work should be done in the modeling of the reaction of chlorine dioxide with VOC mixtures. More reaction kinetic data under different pH levels are necessary to train the ANN in order to improve the model performance for VOC mixtures. For very fast reactions at high pH that are not satisfy the pseudo first-order condition, suitable instrument adjustments, such as using shorter path length cell, are suggested to reduce the instrument noises (Operator's Manual for the SF-61SX2 Stopped-flow System).

A. Changes of Absorptions at 358 nm and 250 nm in the Reaction of ClO_2 with Ethanethiol and

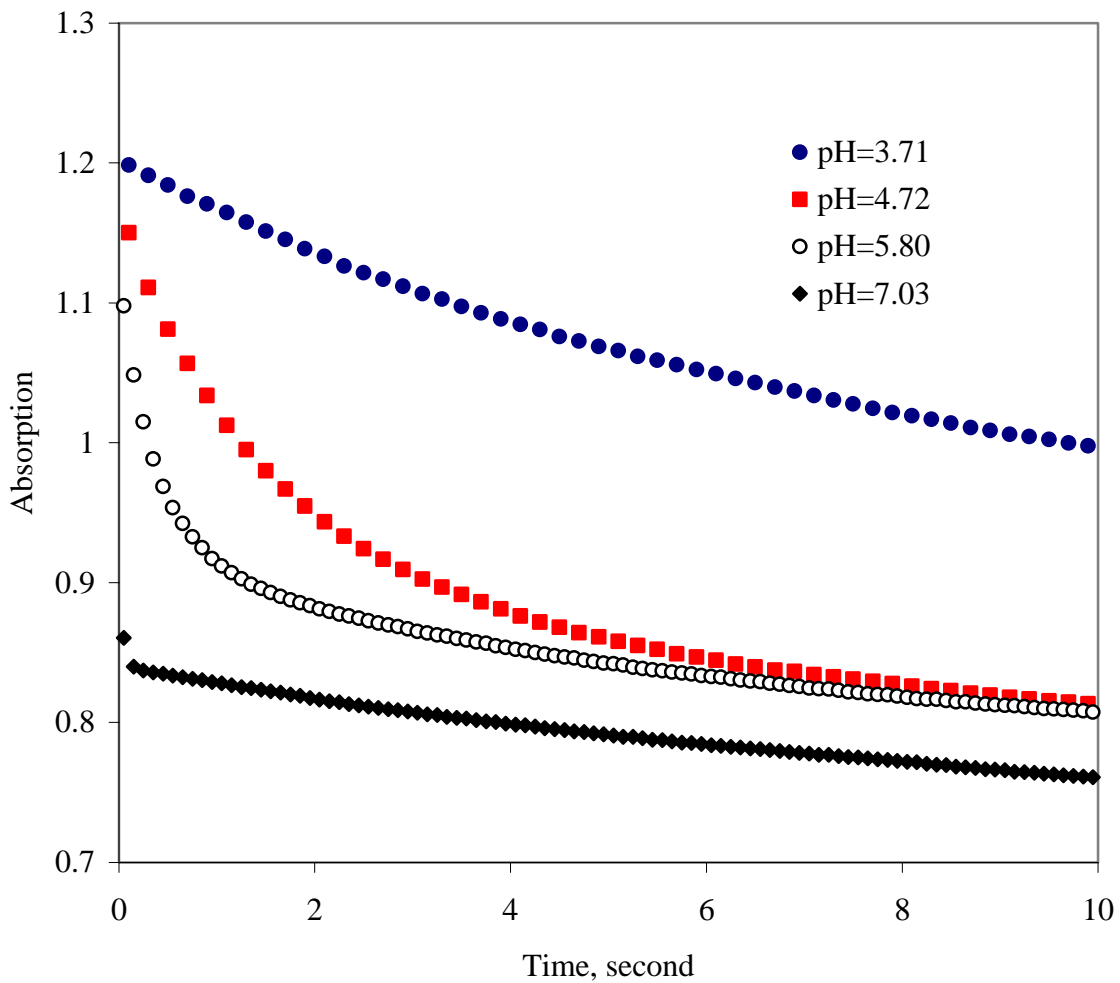DMDS Mixtures at Different pH Levels (An Example)

Fig. A.1 Absorption changes at 358 nm in the reaction of 60 mg/L ClO_2 with 10 mg/L ethanethiol and 10 mg/L DMDS mixtures at 30ºC and different pH levels
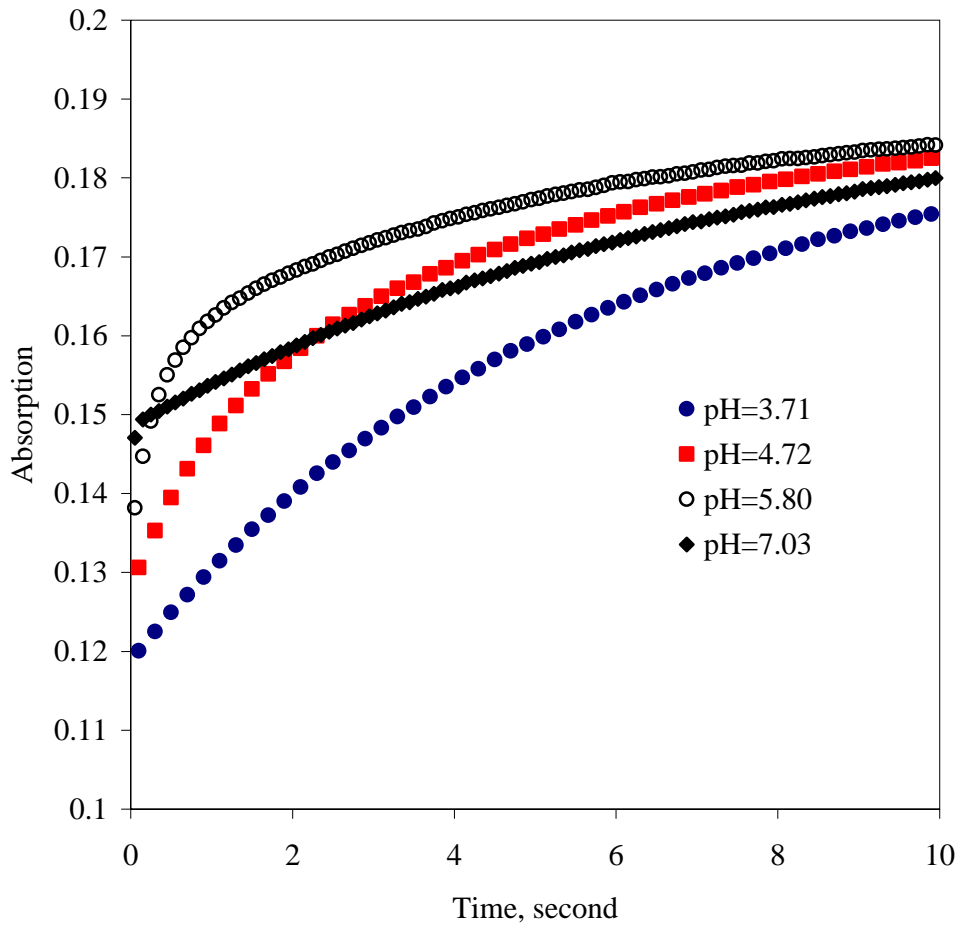
Fig. A.2 Absorption changes at 250 nm in the reaction of 60 mg/L
ClO2 with 10 mg/L ethanethiol and 10 mg/L DMDS mixtures at 30ºC
and different pH levels